Assembly, molecular organization, and membrane-binding properties of development-specific septins

Galo Garcia III,[1]* Gregory C. Finnigan,[1]* Lydia R. Heasley,[2]* Sarah M. Sterling,[1] Adeeti Aggarwal,[1] Chad G. Pearson,[2] Eva Nogales,[1,3,4] Michael A. McMurray,[2] and Jeremy Thorner[1]

[1]Division of Biochemistry, Biophysics, and Structural Biology, Department of Molecular and Cell Biology, University of California, Berkeley, Berkeley, CA 94720
[2]Department of Cell and Developmental Biology, University of Colorado Denver School of Medicine, Aurora, CO 80045
[3]Life Sciences Division, Lawrence Berkeley National Laboratory, Berkeley, CA 94720
[4]Howard Hughes Medical Institute, Chevy Chase, MD 20815

Septin complexes display remarkable plasticity in subunit composition, yet how a new subunit assembled into higher-order structures confers different functions is not fully understood. Here, this question is addressed in budding yeast, where during meiosis Spr3 and Spr28 replace the mitotic septin subunits Cdc12 and Cdc11 (and Shs1), respectively. In vitro, the sole stable complex that contains both meiosis-specific septins is a linear Spr28–Spr3–Cdc3–Cdc10–Cdc10–Cdc3–Spr3–Spr28 hetero-octamer. Only coexpressed Spr3 and Spr28 colocalize with Cdc3 and Cdc10 in mitotic cells, indicating that incorporation requires a Spr28-Spr3 protomer. Unlike their mitotic counterparts, Spr28-Spr3–capped rods are unable to form higher-order structures in solution but assemble to form long paired filaments on lipid monolayers containing phosphatidylinositol-4,5-*bis*phosphate, mimicking presence of this phosphoinositide in the prospore membrane. Spr28 and Spr3 fail to rescue the lethality of a *cdc11*Δ *cdc12*Δ mutant, and Cdc11 and Cdc12 fail to restore sporulation proficiency to *spr3*Δ/*spr3*Δ *spr28*Δ/*spr28*Δ diploids. Thus, specific meiotic and mitotic subunits endow septin complexes with functionally distinct properties.

Introduction

Septins are a family of GTP-binding proteins conserved in all eukaryotes (except higher plants; Pan et al., 2007; Nishihama et al., 2011). In organisms as evolutionarily distant as yeast and humans, septins assemble into a linear hetero-octameric complex composed of four different monomers arranged with two-fold rotational symmetry (Bertin et al., 2008; Kim et al., 2011; Sellin et al., 2012). The resulting apolar rods can self-associate into long filaments and other, more complex higher-order structures. However, the genomes of yeast and humans encode, respectively, seven and thirteen different septins, raising important questions about the number of allowed combinatorial arrangements of these monomers and their respective physiological functions. Moreover, how are certain combinations favored over others when potentially redundant subunits are co-expressed? As we document here, the assembly properties and roles of a development-specific septin complex in yeast now provide important new insights that address these questions. This unique complex is formed during yeast meiosis and sporulation, a process closely akin to mammalian gametogenesis.

On a poor carbon source and limited nitrogen supply, a diploid (*MAT***a**/*MAT*α) *Saccharomyces cerevisiae* cell undergoes meiosis within its own cytoplasm. The resulting four haploid nuclei are encased into spores, surrounded by the old cell wall (ascus; Fowell, 1969; Neiman, 2011). In this process, the nuclear envelope is remodeled, forming four lobes. Each lobe directs assembly of a closely allied membrane (the prospore membrane [PSM]) that becomes the spore plasma membrane, on which are deposited the spore wall and other protective coatings (Maier et al., 2007; Morishita and Engebrecht, 2008). The PSM assembles de novo from vesicles that dock and fuse, initially forming a cup-like cap above each nuclear lobe that expands and engulfs each incipient haploid nucleus (Moens, 1971; Riedel et al., 2005; Nakanishi et al., 2006). A septin-based structure is tightly associated with the developing PSM (De Virgilio et al., 1996; Fares et al., 1996; Pablo-Hernando et al., 2008).

In mitotic cells, five septins are expressed and assemble into two complexes differing only in the terminal subunit: Cdc11–Cdc12–Cdc3–Cdc10–Cdc10–Cdc3–Cdc12–Cdc11 and Shs1–Cdc12–Cdc3–Cdc10–Cdc10–Cdc3–Cdc12–Shs1. Cdc11-

*G. Garcia III, G.C. Finnigan, and L.R. Heasley contributed equally to this paper.

Correspondence to Jeremy Thorner: jthorner@berkeley.edu; Michael A. McMurray: michael.mcmurray@ucdenver.edu; or Eva Nogales: enogales@lbl.gov

G. Garcia III's present address is Dept. of Biochemistry and Biophysics and Cardiovascular Research Institute, University of California, San Francisco, San Francisco, CA 94158.

Abbreviations used in this paper: 5-FOA, 5-fluoro-orotic acid; BiFC, bimolecular fluorescence complementation; CTE, C-terminal extension; DOPC, 1,2-dioleoyl-*sn*-phosphatidylcholine; PSM, prospore membrane.

The Rockefeller University Press $30.00
J. Cell Biol. Vol. 212 No. 5 515–529
www.jcb.org/cgi/doi/10.1083/jcb.201511029

capped rods polymerize end-on-end into straight paired filaments when the salt concentration <150 mM (Bertin et al., 2008; Booth et al., 2015), whereas, under the same conditions, Shs1-capped rods associate laterally, not end to end (Booth et al., 2015), to form spirals and rings (Garcia et al., 2011). In meiotic cells, two new septins, Spr3 (Ozsarac et al., 1995; Fares et al., 1996) and Spr28 (De Virgilio et al., 1996), are produced (Brar et al., 2012). At the transcriptional level, *SPR3*, *SPR28*, *CDC3*, and *CDC10* are induced during meiosis, whereas *CDC11* and *CDC12* are not (Kaback and Feldberg, 1985; Chu et al., 1998), and *SHS1* is repressed (Friedlander et al., 2006). These findings are consistent with a model (McMurray and Thorner, 2008) in which, during meiosis, Cdc11 (and Shs1) and Cdc12 are replaced by Spr28 and Spr3, a pair of potentially interacting subunits, thereby generating a novel hetero-octameric complex unique to sporulating cells.

During sporulation, Spr3, Spr28, Cdc3, and Cdc10 are prominently localized to the PSM, and Cdc11 is detectable (Fares et al., 1996; Pablo-Hernando et al., 2008), whereas the bulk of Cdc12 and Shs1 are excluded from septin structures at the PSM (Douglas et al., 2005; McMurray and Thorner, 2008, 2009). Septins appear first on the nuclear-proximal side of the initial PSM. As the PSM cup expands, a U-shaped septin structure ("horseshoe") forms, whose arms elongate as the PSM closes. After its closure, septins are distributed more evenly on the cytoplasmic face of the spore plasma membrane (Fares et al., 1996; Neiman, 2011).

In an *spr28Δ/spr28Δ* diploid, the horseshoe does not form and the other septins are dispersed over the PSM surface (Pablo-Hernando et al., 2008). In an *spr3Δ/spr3Δ* diploid, the horseshoe is also eliminated and association of other septins with the PSM is greatly reduced (Fares et al., 1996; Pablo-Hernando et al., 2008). Despite these drastic perturbations of normal meiotic septin organization, loss of Spr3 (Kao et al., 1989; Fares et al., 1996) or Spr28 (De Virgilio et al., 1996), or both (Fares et al., 1996; A. Neiman, personal communication), reportedly caused little, if any, reduction in spore formation.

In this study, we sought to determine how Spr3 and Spr28 contribute to overall septin architecture at the ultrastructural level and to examine both in vitro and in vivo the biochemical and biophysical properties of the complexes that contain them, especially their interaction with membranes. We also reinvestigated the phenotype of cells lacking Spr3 and Spr28 and found, contrary to prior studies, that absence of either of these septins markedly reduces sporulation proficiency, as documented here, as well as compromises the structural integrity of the spores that do manage to form, as described in detail elsewhere (Heasley and McMurray, 2016). Our findings provide novel insights about how alternative subunits endow septin complexes with unique properties.

Results

Expression and purification of recombinant septin complexes containing Spr3 and Spr28

In meiotic cells, Spr3 might replace Cdc12 and Spr28 might replace Cdc11 and Shs1, the subunits they most resemble (Fig. S1 and Table S1), thereby generating a unique septin complex with properties specific for execution of sporulation (Fig. 1 A). Analogously, as documented before (Garcia et al., 2011), in mitotic cells, Shs1 competes with and can substitute for Cdc11, its closest paralogue (Fig. S1 and Table S1), yet it accords very different properties on the resulting hetero-octamers.

To ascertain whether Spr3 and Spr28 possess an intrinsic ability to replace their mitotic counterparts, we expressed the sporulation-specific septins as recombinant proteins in bacterial cells alone, together, and with various combinations of the other five septin subunits. Expression of $(His)_6$Cdc12 and untagged versions of Cdc3, Cdc10, and Cdc11 (or Shs1) reproducibly yields stoichiometric complexes of the mitotic septins because Cdc12 is the limiting subunit. Hence, we used $(His)_6$Spr3 in the same way because of its resemblance to Cdc12 and the existing evidence that Spr3 may displace Cdc12 in meiotic cells (McMurray and Thorner, 2008). When $(His)_6$Spr3 was coexpressed with Cdc3 and Cdc10, the three proteins consistently copurified in a stoichiometric complex even in high salt (Fig. 1 B, left, lane 1). When examined by size-exclusion chromatography, the particles in such preparations eluted very similarly to a known septin hetero-hexamer (Fig. 1 C). However, when diluted, dispersed on carbon-coated grids, and viewed under EM (Fig. 1 D), only a minority of the observed rods were hetero-hexamers (mainly pentamers and tetramers were found), indicating that Spr3 had dissociated from one or both ends, suggesting that the Spr3–Cdc3 junction is not very stable.

Next, we coexpressed Spr28 with $(His)_6$Spr3, Cdc3 and Cdc10 and found that these four proteins consistently copurified in a stoichiometric complex even in high salt (Fig. 1 B, left, lane 2). When viewed using EM (Fig. 1 E), or when examined by size-exclusion chromatography against appropriate standards (Fig. 1 C), rods of appropriate length to be hetero-octamers were observed (as well as some of heptamer and hexamer length). By this criterion, presence of Spr28 stabilized the Spr3–Cdc3 interaction. Thus, in vitro, Spr3 and Spr28 together had the capacity to associate with the ends of Cdc3–Cdc10–Cdc10–Cdc3 hetero-tetramers to form Spr28–$(His)_6$Spr3–Cdc3–Cdc10–Cdc10–Cdc3–$(His)_6$Spr3–Spr28 hetero-octamers.

A potential explanation for the observed localization of some Cdc11 on the PSM might be that Spr3 bears sufficient resemblance to Cdc12 that Cdc11–Spr3–Cdc3–Cdc10–Cdc10–Cdc3–Spr3–Cdc11 hetero-octamers are able to form. However, when Cdc11 was coexpressed with $(His)_6$Spr3, Cdc3 and Cdc10, no detectable Cdc11 was incorporated into the resulting complexes, which contained only $(His)_6$Spr3, Cdc3 and Cdc10 (Fig. 1 B, right, lane 2). Another possibility is that Spr28 retains enough similarity to Cdc11 to form a Cdc11–Spr28 junction, in analogy to the Cdc11–Cdc11 interface responsible for the end-to-end polymerization of mitotic Cdc11–Cdc12–Cdc3–Cdc10–Cdc10–Cdc3–Cdc12–Cdc11 rods (Bertin et al., 2008). However, when Cdc11 was coexpressed with Spr28, $(His)_6$Spr3, Cdc3 and Cdc10, no detectable Cdc11 was incorporated into the complexes, which contained only Spr28, $(His)_6$Spr3, Cdc3, and Cdc10 (Fig. 1 B, right, lane 3). Thus, Cdc11 may be present at the PSM as a monomer (or, perhaps, in residual intact mitotic septin complexes that manage to survive during sporulation).

Subunit architecture in sporulation-specific septin complexes

As an independent means to determine the subunit arrangement in the complexes containing Spr3 and Spr28, we performed single-particle analysis. Large numbers of individual particles on EM grids were sorted into groups (classes) on the basis of shared distinctive features. The particles in each class were computationally aligned and averaged to produce a representative

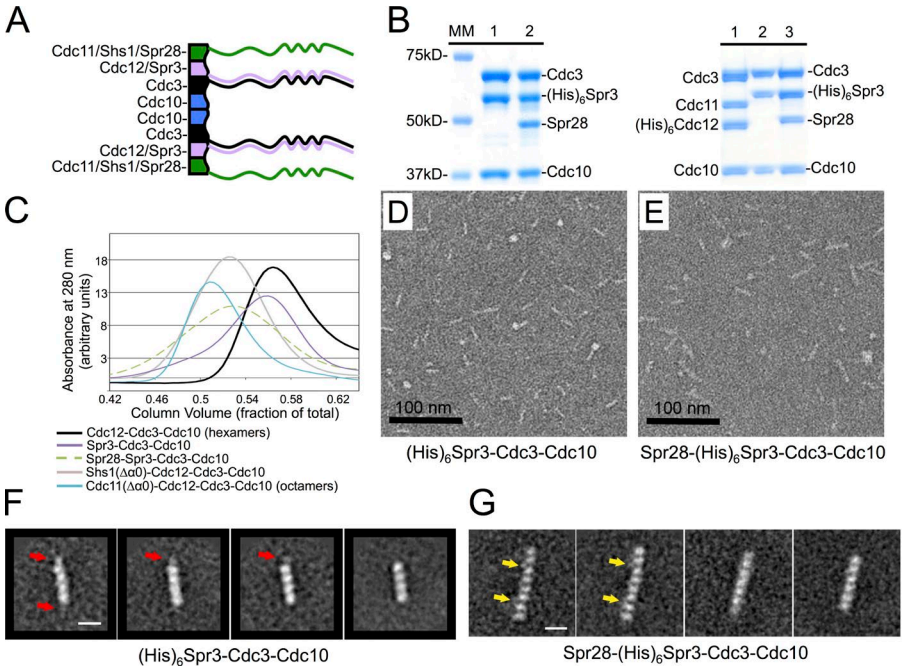

Figure 1. **The sporulation-specific septin complex is a hetero-octameric rod.** (A) Model for organization of the sporulation-specific septin complex and its relationship to mitotic septin complexes. Adjacent monomers in linear septin complexes interact by two alternating contact modes, a G interface (involving residues in and around the GTP-binding pockets), and an NC interface (involving residues in and around the N- and C-terminal segments of the GTP-binding domains). Short side, G interface; long side, NC interface; wavy line, CTE; squiggle, coiled coil. (B) Septins were coexpressed in *E. coli*, the resulting $(His)_6$Spr3-containing complexes were purified as described in Materials and methods, and proteins in the final purified fraction were resolved by SDS-PAGE and visualized by staining with Coomassie blue dye. (left) MM, molecular mass standards; lane 1, Cdc3 and Cdc10 coexpressed with $(His)_6$Spr3; lane 2, Cdc3, Cdc10, and Spr28 coexpressed with $(His)_6$Spr3. (right) Lane 1, Cdc3, Cdc10, and Cdc11 coexpressed with $(His)_6$Cdc12 (mitotic septin complexes); lane 2, Cdc3, Cdc10, and Cdc11 coexpressed with $(His)_6$Spr3; lane 3, Cdc3, Cdc10, Cdc11, and Spr28 coexpressed with $(His)_6$Spr3. (C) Analytical scale size-exclusion chromatography of septin complexes. Cyan, Cdc11(Δα0)-$(His)_6$Cdc12–Cdc3–Cdc10 hetero-octamers; the Δα0 mutation does not prevent rod assembly but blocks its end-to-end polymerization in solution (Bertin et al., 2008); gray, Shs1(Δα0)-$(His)_6$Cdc12–Cdc3–Cdc10 complexes, which represent a mixture of octamers, heptamers, and hexamers (Garcia et al., 2011); green and dashed, Spr28– $(His)_6$Spr3–Cdc3–Cdc10 complex; purple, $(His)_6$Spr3-Cdc3-Cdc10 complex; and black, $(His)_6$Cdc12–Cdc3–Cdc10 complexes, which are stable hetero-hexamers (Bertin et al., 2008). Slightly earlier elution of the $(His)_6$Spr3-Cdc3-Cdc10 complex versus the $(His)_6$Cdc12–Cdc3–Cdc10 complex is attributable to the higher molecular mass of Spr3 (59.8 kD) compared with Cdc12 (46.7 kD). EM images of the complexes from B, left, lane 1 (D) and lane 2 (E) in high-salt buffer, stained with uranyl formate. Globular particles are a contaminant, endogenous *E. coli* ArnA (formerly PmrI), a 70 kD Ni^{2+}-binding polypeptide that copurifies with septin complexes to a variable extent from preparation to preparation because it forms two stacked trimers whose molecular mass is close to that of septin complexes (which, because of their rod shape, elute at a larger apparent size and are not well resolved from the ArnA homohexamer). Bar, 100 nm. (F) Four representative class averages for the $(His)_6$Spr3–Cdc3–Cdc10 complex in high salt. Red arrows show presence of partially unfolded or highly mobile Spr3 indicated by the extra density at the ends of the Cdc3–Cdc10–Cdc10–Cdc3 hetero-tetrameric rods. Bar, 10 nm. (G) Four representative class averages for the Spr28– $(His)_6$Spr3–Cdc3–Cdc10 complex in high salt. Yellow arrows, extra lateral densities representing either a coiled-coil interaction between the CTEs of Spr3 and Cdc3 or the N-terminal domain of Spr3. Bar, 10 nm.

image (class average). The class averages of the complexes composed of $(His)_6$Spr3, Cdc3 and Cdc10 were rod-shaped and had no additional density along the sides of the rod (Fig. 1 F). Given the stoichiometric complexes isolated (Fig. 1 B, left, lane 1) and their hydrodynamic behavior (Fig. 1 C), it was unexpected that a majority were tetrameric (Fig. 1 F, right-most panel). There were, however, classes that appeared pentameric (Fig. 1 F, middle two panels) and hexameric (Fig. 1 F, left-most panel) because they contained additional, albeit weak, density at one or both ends the rod. This behavior indicates that association of Spr3 with Cdc3 is relatively weak, that the terminal Spr3 molecules unfold relatively easily, or that Spr3 is attached via a linkage that allows for significant flexibility. In analogy to the Cdc12–Cdc3 interaction, Spr3 likely associates with Cdc3 via both its globular domain and via formation of a coiled coil between its C-terminal extension (CTE) and that of Cdc3 (Fig. 1 C). If the latter interaction is stronger and more mobile, it might explain the relatively weak end densities observed.

Class averages of complexes composed of Spr28, $(His)_6$Spr3, Cdc3 and Cdc10 were also rod-shaped (Fig. 1 G), and the majority were clearly octameric (Fig. 1 G, left-most two panels); out of 1,990 total rods counted, 972 (49%) were octamers, 335 (17%) heptamers, and 683 (34%) hexamers. In the octamers, the penultimate protomer displayed a density as prominent as any other subunit, consistent with stabilization of Spr3 via its association with Spr28. The octamers contained a conspicuous density located between the second and third subunits (Fig. 1 G, left two panels) and situated on the same side of the rod. The CTEs at each NC interface in mammalian septin rods form coiled coils (de Almeida Marques et al., 2012) and, in their native state, must extend from the same side of the rod (Sirajuddin et al., 2007). Thus, the observed densities could represent a coiled coil between the CTEs of Spr3 and Cdc3 (Fig. 1 C). Alternately, this extra density could represent a stable fold adopted by the unique N-terminal domain in Spr3, which is 75 residues longer than that in Cdc12 (Fig. 1 A). Heptameric (Fig. 1 G, second panel from the right) and hexameric (Fig. 1 G, right-most panel) classes presumably arose from dissociation of Spr28 from one or both ends. Thus, Spr28 occupies the terminal position and Spr3 occupies the penultimate position in the hetero-octamers.

Higher-order assembly of sporulation-specific septin complexes

When diluted from high to low salt and deposited from solution onto EM grids, mitotic Cdc11–Cdc12–Cdc3–Cdc10–Cdc10–Cdc3–Cdc12–Cdc11 hetero-octamers have polymerized into long paired filaments (Bertin et al., 2008; Fig. 2 A, left). When treated in the same manner, neither Spr28–Spr3–Cdc3–Cdc10–Cdc10–Cdc3–Spr3–Spr28 hetero-octamers (Fig. 2 B, middle) nor Spr3–Cdc3–Cdc10–Cdc10–Cdc3–Spr3 hetero-hexamers (Fig. 2 A, right) formed any higher-order structure. The lack of

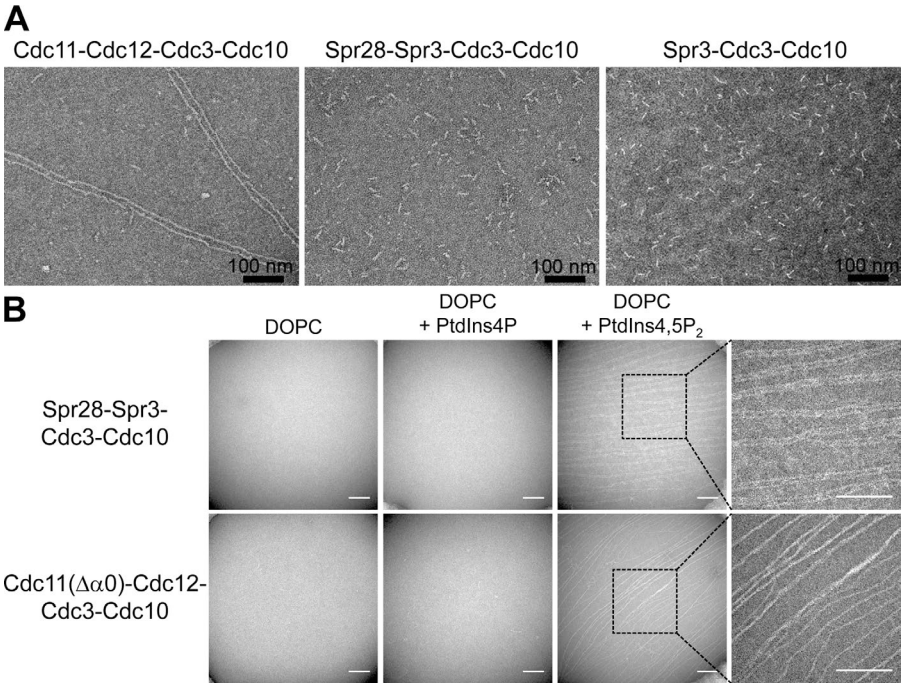

Figure 2. **PtdIns4,5P_2 promotes assembly of sporulation-specific septin complexes.** (A) The indicated septin complexes were diluted from high-salt buffer into low-salt buffer, incubated for 1 h, deposited on grids, stained with uranyl formate, and viewed by EM. Left, Cdc11–$(His)_6$Cdc12–Cdc3–Cdc10–Cdc10–Cdc3-$(His)_6$Cdc12–Cdc11 (mitotic) hetero-octamers; middle, Spr28– $(His)_6$Spr3–Cdc3–Cdc10–Cdc10–Cdc3–$(His)_6$Spr3–Spr28 hetero-octamers; right, $(His)_6$Spr3–Cdc3–Cdc10–Cdc10–Cdc3–$(His)_6$Spr3 hetero-hexamers. (B) The sporulation-specific septin complex (top) and a control mitotic septin complex (bottom) whose polymerization into filaments is promoted on the surface of a PtdIn4,5P_2-containing lipid monolayer (Bertin et al., 2010) were diluted into low-salt buffer in a droplet, whose meniscus was overlaid with a solution of a monolayer-forming lipid containing DOPC alone, DOPC containing PtdIns4P, or DOPC containing PtdIns4,5P_2, as indicated. Any proteins associated with the headgroups of the lipid monolayer were visualized by capturing its hydrophobic side by binding to a holey carbon-coated grid, staining with uranyl formate, and inspecting the regions of the monolayer that span holes in the grid by EM. Right-most panels, magnified views of the indicated insets. Bar, 100 nm.

observable self-assembly could indicate that sporulation-specific complexes are incapable of self-association or, if a higher-order structure forms, it is very fragile. Alternatively, the solution conditions chosen may not be suitable for interaction, or a molecular partner present in meiotic cells, but absent in our purified preparations, is necessary to promote higher-order assembly.

In the latter regard, the PSM in *S. cerevisiae* is highly enriched in PtdIns4,5P_2, and production of this phosphoinositide is essential for sporulation (Rudge et al., 2004; Park and Neiman, 2012). Moreover, presence of PtdIns4,5P_2 (and no other phosphoinositide) promotes polymerization of mitotic septin complexes on a lipid monolayer under high-salt conditions that do not permit filament formation in solution (Bertin et al., 2010). Similarly, mitotic septin complexes capped with Cdc11(Δα0), a mutation that weakens the Cdc11–Cdc11 interaction, do not form filaments in low-salt solution (Bertin et al., 2008) but readily form filaments on the surface of the PtdIns4,5P_2-containing monolayer (Bertin et al., 2010).

For these reasons, we tested whether sporulation-specific septin complexes would display higher-order assembly when confronted with a PtdIns4,5P_2-containing monolayer. Control lipid monolayers composed of 1,2-dioleoyl-*sn*-phosphatidylcholine (DOPC) alone, as well as DOPC doped with 15 mol% PtdIns4P, were unable to recruit either the Spr28–Spr3–Cdc3–Cdc10–Cdc10–Cdc3–Spr3–Spr28 complex (Fig. 2 B, top) or the Cdc11(Δα0)–Cdc12–Cdc3–Cdc10–Cdc10–Cdc3–Cdc12–Cdc11(Δα0) complex (Fig. 2 B, bottom) to their surface, even from low salt buffer. In marked contrast, DOPC doped with 15 mol% PtdIns4,5P_2 robustly recruited both the sporulation-specific septin complex (Fig. 2 B, top) and the mutant mitotic septin complex (Fig. 2 B, bottom) to the surface and promoted formation of prominent and well-ordered filaments. Enlargement revealed that the filaments generated by the sporulation-specific septin complex are paired and laterally connected by an obvious "rungs-on-a-ladder" cross-bracing (Fig. 2 B, top), whereas many of the filaments generated by the mutant mitotic septin complex are in tight pairs (Fig. 2 B, bottom), as seen before (Bertin et al., 2010). Thus, PtdIns4,5P_2 profoundly affected the assembly state of Spr28–Spr3–Cdc3–Cdc10–Cdc10–Cdc3–Spr3–Spr28 hetero-octamers.

Sporulation-specific septins cannot support mitotic growth

To test whether Spr28 and Spr3 can functionally substitute for Cdc11 and Cdc12, respectively, the sporulation-specific septins (marked with fluorescent tags) were integrated into the genome under control of the *CDC11* and *CDC12* promoters at their endogenous loci. The strains also carried *URA3*-marked plasmids that expressed a wild-type copy of the mitotic septin gene that was replaced with its sporulation-specific counterpart. Just like a *cdc11Δ* mutant, the cells harboring the integrated *$CDC11_{prom}$-SPR28-GFP* construct were unable to propagate when the *URA3*-marked *CDC11*-expressing plasmid was selected against on medium containing 5-fluoro-orotic acid (5-FOA; Fig. 3 A, second and fourth lanes). Likewise, just like a *cdc12Δ* mutant, the cells harboring the integrated *$CDC12_{prom}$-SPR3-mCherry* construct were unable to grow on 5-FOA medium (Fig. 3 A, third and fifth lanes). This latter finding agrees with the results of Fares et al. (1996) who showed that ectopic expression of Spr3 was unable to rescue growth at the nonpermissive temperature of strains carrying a *$cdc3^{ts}$*, *$cdc10^{ts}$*, *$cdc11^{ts}$*, or *$cdc12^{ts}$* allele. In our hands, even presence of both *$CDC11_{prom}$-SPR28-GFP* and *$CDC12_{prom}$-SPR3-mCherry* was unable to rescue the inviability of a *cdc11Δ cdc12Δ* double mutant (Fig. 3 A, line 6). Lack of complementation was not caused by lack of expression, as both sporulation-specific septins were stably produced in these cells at levels similar to tagged versions of Cdc11 and Cdc12, as confirmed by visualization of the cells (Fig. 3 B) and by immunoblotting (Fig. 3 D). Thus, the sporulation-specific subunits cannot functionally replace the corresponding mitotic septins.

In vegetative cells, either Cdc11-GFP (Fig. 3 B, left, top) or Cdc12-GFP (Fig. 3 B, left, bottom) were quantitatively in-

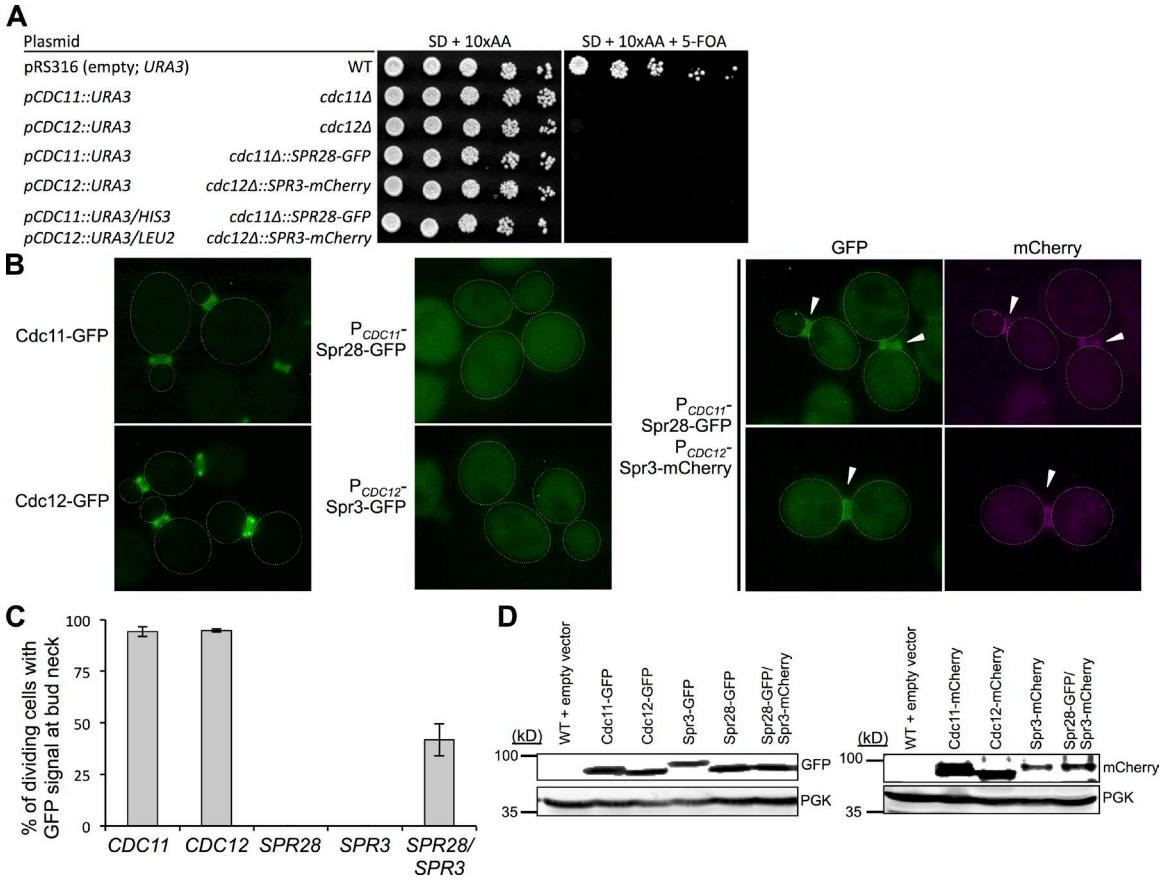

Figure 3. **Spr3 and Spr28 do not functionally substitute for Cdc12 and Cdc11 in vegetative cells and are competent to associate with mitotic septins only when coexpressed.** (A) Haploid cells of the indicated genotype (middle column) and containing a *URA3*-marked plasmid (left column) expressing wild-type *CDC11* or wild-type *CDC12*, or both (to ensure viability) were grown in selective (–Ura) medium and then serially diluted onto control medium (synthetic complete; left) or the same medium containing 5-FOA to select against the *URA3*-marked covering plasmid (right). Where indicated, sporulation-specific septins *SPR28-GFP* and *SPR3-mCherry* were expressed from the *CDC11* and *CDC12* promoters, respectively, at the corresponding chromosomal loci. (B) Otherwise wild-type cells expressing the indicated fluorescently-tagged septins were grown to mid-exponential phase in YPD and visualized by fluorescence microscopy. Faint dotted white lines, yeast cells periphery; arrowheads, fluorescent signal at the bud neck. Bar, 2 µm. (C) Quantification of B. Hundreds of cells in independent cultures expressing tagged Spr28 alone (n = 3), tagged Spr3 alone (n = 3), or both (n = 5) were examined by fluorescence microscopy. Bars, mean percentage of the budded cells that displayed a visible fluorescent signal at the bud neck; error bar, standard deviation of the mean. (D) To analyze expression of the indicated fluorescently tagged septins in the cells from B (left) and Fig. S1 (right), equivalent numbers of cells were lysed, resolved by SDS-PAGE, transferred to a nitrocellulose filter, and probed with appropriate antibodies (anti-GFP, anti-DsRed, or anti-Pgk1). Pgk1, control for equivalent protein loading.

corporated into the filamentous collar at the bud neck, whereas Spr28-GFP (Fig. 3 B, middle, top) and Spr3-GFP (Fig. 3 B, middle, bottom) each displayed only cytosolic fluorescence in all cells examined. Revealingly, however, in cells coexpressing Spr28-GFP and Spr3-mCherry (Fig. 3 B, right), a significant proportion of the dividing cells (40–45%; Fig. 3 C) exhibited a clearly detectable fluorescent signal for both proteins at the bud neck, in addition to the diffuse cytosolic fluorescence (Fig. 3 B, right), even though the cells also expressed all five mitotic septins. Similar results were obtained when the fluorescent tags were swapped (Spr28-mCherry and Spr3-GFP; Fig. S2). Thus, in the cytoplasm of a mitotic cell, the sporulation-specific septins are competent for association with other septin subunits. Hence, the inability of Spr28 and Spr3 to complement *cdc11Δ* and *cdc12Δ* mutations, respectively, cannot be attributed to misfolding of these proteins. Second, incorporation of Spr28 and Spr3 at the bud neck in vivo required their simultaneous presence. Thus, the two proteins function as a unit and mutually promote their assembly into hetero-octamers, consistent with the conclusions of our in vitro biochemical and EM findings.

As shown here, Spr3 shares with Cdc12 the capacity to interact with Cdc3, and sporulation-specific hetero-octamers share with mitotic septin hetero-octamers the capacity to bind PtdIns4,5P_2. Hence, expression of Spr3 and Spr28 in mitotic cells could interfere with normal growth. When Spr28-GFP was produced from the *CDC11* promoter on a *CEN* vector, or Spr3-mCherry was made from the *CDC12* promoter on another *CEN* vector (or both), there was no obvious effect on the growth rate of otherwise wild-type cells (Fig. S3). However, when we used any of three different means to ectopically over-produce the sporulation-specific septins in vegetative cells that also carried sensitizing mutations (alleles that compromise the function of particular septin subunits), mitotic growth rate was markedly reduced (Fig. S4) and cell morphology was altered in an increased proportion of the cell population (Fig. S5).

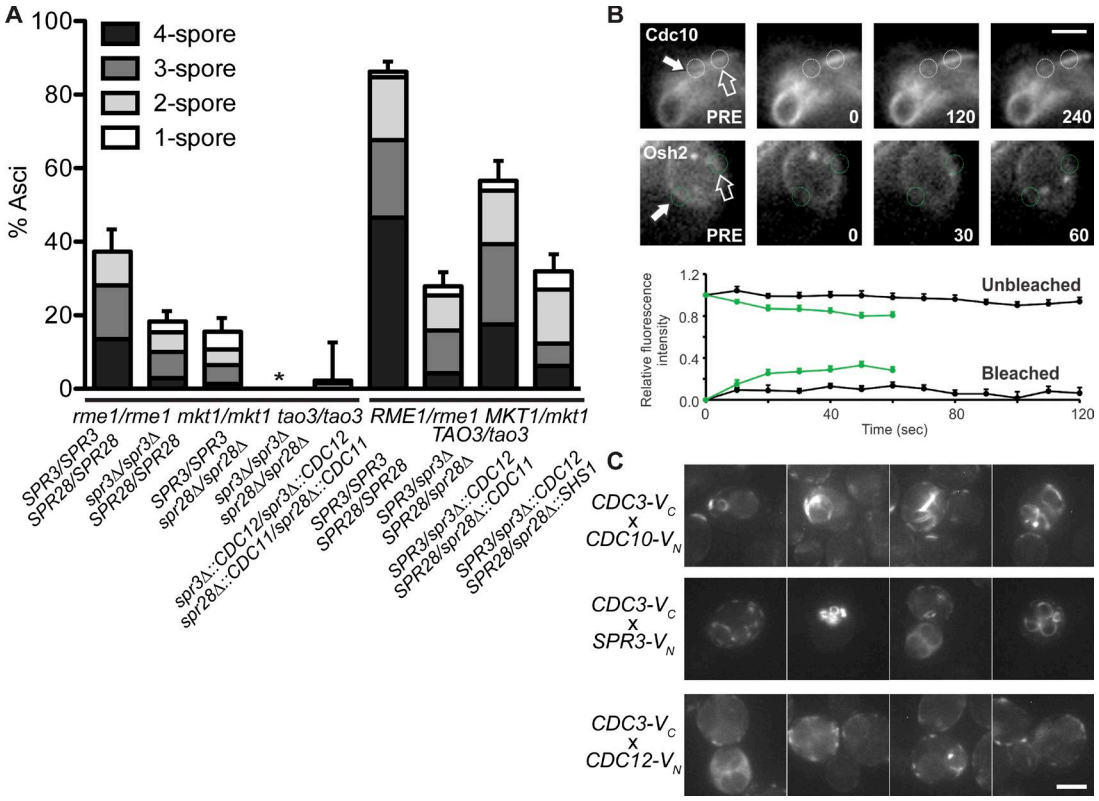

Figure 4. **Spr3- and Spr28-containing complexes are required for septin function and localization during sporulation.** (A) Overall sporulation efficiencies and spore number per ascus were determined for diploids of the indicated genotypes. Left side, BY4743; MMY0221; MMY0154; MMY0231; GCFY7. The left-most three columns recapitulate data in Heasley and McMurray (2016) are included as a basis for comparison to the effect on sporulation proficiency of loss of both *SPR3* and *SPR28* or of replacing them with *CDC12* and *CDC11*, respectively. Right side, MMY0228, MMY0184 x MMY0155; MMY0230; MMY0226. Asterisk, no asci detectable; error bars, standard error of the proportion. (B) FRAP analysis. Top micrograph, representative Cdc10-GFP-expressing cell; bottom micrograph, representative GFP-2X(PH^{Osh2})-expressing cell. Dashed circles, sites of signal bleaching and/or detection; filled white arrow, bleached site; outlined dark arrow, unbleached (control) site. Bar, 2 µm. (bottom) Cdc10-GFP-marked septin structures (black lines) or GFP-2X(PH^{Osh2})–marked portions of the PSM (green lines) were photobleached and recovery was visualized by time-course imaging, quantified, averaged over all trials, and plotted as the mean ± SEM. Top lines, unbleached (control) area; bottom lines, bleached area. Mean percent recovery: Cdc10-GFP, 9.4 ± 2.9% (n = 15); GFP-2X(PH^{Osh2}), 28.4 ± 2.9% (n = 11). (C) Representative images of YFP fluorescence in sporulating cells expressing the indicated BiFC pairs. Bar, 5 µm.

Mitotic septins alone cannot support sporulation

In the BY4743 genetic background (Brachmann et al., 1998), the homozygous *spr3Δ/spr3Δ* and *spr28Δ/spr28Δ MAT***a**/*MAT*α diploids we constructed exhibited a marked reduction in overall sporulation proficiency, especially in production of four-spored asci, compared with the otherwise isogenic parental diploid (Fig. 4 A, left). Similarly, in a high-throughput screen (Enyenihi and Saunders, 2003), severe sporulation defects were seen in the absence of *CDC10* in BY4743 cells. Moreover, diploid cells lacking both *SPR3* and *SPR28* failed to generate any detectable spores (Fig. 4 A, left). Importantly, in diploids in which the mitotic septins Cdc11 and Cdc12 were expressed from the native *SPR28* and *SPR3* promoters in place of the corresponding sporulation-specific septins, sporulation proficiency was scarcely increased (Fig. 4 A, left). Similarly, in the background of a hybrid between BY4743 and the SK1 strain typically used for synchronous and highly efficient meiosis (Börner and Cha, 2015) that was constructed and characterized (Heasley and McMurray, 2016), sporulation efficiency is very sensitive to the dose of Spr3 and Spr28 present and not fully restored by meiosis-specific expression of either Cdc12 and Cdc11 or Cdc12 and Shs1 (Fig. 4 A, right). Thus, just as Spr3 and Spr28 cannot functionally replace Cdc12 and Cdc11 to support mitosis, these mitotic septin subunits cannot functionally replace their meiosis-specific counterparts in the sporulation process.

Behavior of sporulation-specific septin complexes in vivo

One characteristic of septins stably assembled into filaments and higher-order structures in mitotic cells is a markedly diminished mobility, as judged by a lack of FRAP in cells expressing fluorescently-tagged septins (Caviston et al., 2003; Dobbelaere et al., 2003). Given that PtdIns4,5P_2 is highly enriched in the PSM, and our observation that this lipid promotes polymerization of the Spr28–Spr3–Cdc3–Cdc10–Cdc10–Cdc3–Spr3–Spr28 complex into filaments in vitro (Fig. 2 B), we used FRAP to determine whether the septin-containing "horseshoes" observed by light microscopy in sporulating cells display the FRAP behavior expected for a highly organized array of filaments. We found that the structures containing Cdc10-GFP never exhibited significant recovery of their fluorescent signal (<10%; n = 15) after photobleaching (Fig. 4 B, top), whereas areas bleached of GFP-2X(PH^{Osh2}), a probe that binds to PtIns4P (a hydrolysis product of PtdIns4,5P_2) on membranes (Roy and Levine, 2004), displayed substantially greater recovery of the fluorescent

signal (22–55%, depending on the experiment; $n = 11$; Fig. 4 B, bottom). Thus, as assessed by FRAP, the septin-containing structures on the PSM display in vivo the hallmark of highly organized structures, consistent with their PtdIns4,5P_2-promoted assembly into well ordered filaments in vitro.

We demonstrated before that the premade Cdc12 and Shs1 persist during sporulation, but are localized mainly in the ascal cytoplasm and not associated with the other septins (McMurray and Thorner, 2008), suggesting that their replacement by Spr3 and Spr28 may involve an active process for their eviction. We reasoned that if we could overcome this eviction mechanism by forcing stable interaction between Cdc12 and Cdc3, we could assess the consequences of maintaining some mitotic-like septin complexes in sporulating cells. To achieve this end, we used bimolecular fluorescence complementation (BiFC) because, once two associating proteins bring the two halves of the fluorescent reporter protein together, they are irreversibly "locked" together (Kerppola, 2008). As a control, we first coexpressed Cdc3-V_C with Cdc10-V_N, which we anticipated should fluorescently mark the septin horseshoes associated with the developing PSMs, as we indeed observed (Fig. 4 C, top). Likewise, we expected that when Cdc3-V_C was coexpressed with Spr3-V_N, only septin structures associated with developing PSMs would yield a prominent signal, as we also observed (Fig. 4 C, middle). In contrast, in sporulating cells containing Cdc3-V_C and Cdc12-V_N, most of the fluorescence was located in small puncta dispersed around the periphery of the ascus and not associated with PSMs at all (Fig. 4 C, bottom). Thus, presence of Cdc12 in septin complexes is not compatible with their ability to form the PSM-associated septin structures required for sporulation. These findings explain why, during meiosis, replacement of Cdc12 by Spr3 is critical for the formation the septin architecture necessary for proper execution of this developmental process.

Discussion

In phylogenetic comparisons of evolutionary relationships among septins (Pan et al., 2007; Momany et al., 2008; Nishihama et al., 2011), *S. cerevisiae* Spr28 is most closely related to Cdc11-like subunits and *S. cerevisiae* Spr3 is most closely related to Cdc12-like subunits. Such trees also indicate that Spr28 diverged before the split that separates the Cdc11-like group from its closest relative, the Shs1-like group. Moreover, Spr-like homologues, even in yeasts closely related to *S. cerevisiae*, are quite divergent (i.e., there is substantial sequence variation among Spr family members but strong conservation of Cdc11 and Cdc12 identity among the same species), suggesting that Spr subunit structure is not highly constrained. Nonetheless, we found that *S. cerevisiae* Spr3 and Spr28 each replace their closest mitotic septin relatives, thereby forming a linear sporulation-specific Spr28–Spr3–Cdc3–Cdc10–Cdc10–Cdc3–Spr3–Spr28 complex with unique assembly and membrane-localizing properties. Thus, our findings reveal how displacement of resident septins by alternative subunits can confer distinctive supramolecular organization and function on septin complexes.

During sporulation in fission yeast (*Schizosaccharomyces pombe*), three new septins (Spn5, Spn6, and Spn7) assemble with Spn2 (Longtine et al., 1996) and supplant the vegetatively expressed septins (Spn1, Spn3, and Spn4) that associate with Spn2 (An et al., 2004). The three sporulation-specific subunits form a complex with Spn2 in vitro (although their order/organization has not been determined) and colocalize interdependently in vivo to the forespore membrane (equivalent to the PSM in *S. cerevisiae*), and loss of a sporulation-specific subunit results in less organized forespore membrane growth and decreases the number of viable spores formed (Onishi et al., 2010). Spn7 is most similar to Spr28 and Spn6 is most closely related to Spr3. Absence of Spn7 prevents incorporation of Spn6 into complexes with the other two septins (Onishi et al., 2010), similar to our observation that presence of both Spr28 and Spr3 promotes their mutual incorporation into hetero-octamers. The ability of coexpressed Spr28 and Spr3 to contribute to formation of hetero-octamers that are stable to EM processing in vitro and to incorporate into the bud neck in mitotic cells (when neither alone is competent to do so) suggests that they form a heterodimer in which Spr28 confers on Spr3 sufficient stability and affinity for Cdc3 to successfully compete with Cdc11-Cdc12. Perhaps all septin pairs, like Spr28-Spr3, first interact via their G interfaces forming a heterodimer before they assemble via their NC interfaces into hetero-octamers (Sirajuddin et al., 2007; Bertin et al., 2008; Weirich et al., 2008), akin to conclusions about the formation of mammalian septin complexes reached by Kim et al. (2012).

A striking feature of the sporulation-specific hetero-octamers was lack of self-association in low-salt solution. However, on lipid monolayers containing PtdIns4,5P_2 as a plasma membrane mimic, sporulation-specific hetero-octamers were able to polymerize end-on-end into long paired filaments with a pronounced "railroad track" appearance and aligned extensively in rather well-organized parallel arrays. A basic motif in the so-called α0 helix just upstream of the conserved P-loop of the GTP-binding domain has been implicated in the ability of a septin subunit to interact with PtdIns4,5P_2 (Zhang et al., 1999). In this regard, Spr3 is slightly more basic in this region (RELLNAKN) than Cdc12 (RYKIVNEE; Fig. S1 A), and Spr28 has just as many basic residues (six) in this region as does Cdc11 or Shs1 (Fig. S1 B). The corresponding basic patches in Cdc10, Cdc11 and Shs1 are necessary for membrane recruitment and function of these proteins (Finnigan et al., 2015).

In *S. pombe*, the forespore membrane is enriched in PtdIns4P, and two sporulation-specific septin subunits (Spn2 and Spn7) bind this phosphoinositide (Onishi et al., 2010). Cells expressing a Spn2 mutant unable to bind PtdIns4P still form septin complexes, but they fail to associate with the forespore membrane, which becomes disoriented, suggesting that septin binding to the forespore membrane helps guide its oriented growth (Onishi et al., 2010). Similar to what we show here for *S. cerevisiae* sporulation-specific septin complexes, recombinant *S. pombe* sporulation-specific septin complexes do not form filaments in solution (M. Onishi, personal communication). However, for *S. cerevisiae* sporulation-specific septin complexes, it is PtdIns4,5P_2, not PtdIns4, that promotes formation of ordered filament ensembles. Our results further highlight the importance of phosphoinositides in regulating septin assembly and organization.

Although others reported that diploids lacking Spr3 (Fares et al., 1996) or Spr28 (De Virgilio et al., 1996) display only a mild, if any, decrease in the efficiency of sporulation compared with corresponding control cells, we found an obvious and severe reduction in sporulation proficiency in the absence of either of the sporulation-specific septins in BY4743 diploids. We also observed the same in a BY-SK1 hybrid strain (Heasley

and McMurray, 2016) that displays an overall higher sporulation efficiency. Aside from the fact that we took great care to always use a uniform sporulation protocol, we have no obvious explanation for why, in our hands, diploids lacking Spr3 and/or Spr28 have a more profound phenotypic effect on sporulation than was previously described by others.

It is clear from our genetic complementation tests that Spr3 and Spr28 cannot substitute for the essential functions of Cdc12 and Cdc11 in mitotic cells; conversely, Cdc12 and Cdc11 cannot perform the function(s) executed by Spr3 and Spr28 in meiotic cells. In the latter regard, when Spr3 or Spr28 are absent, there is at least a 10-fold reduction in the frequency of sporulation. Also, the fitness of the few spores that are produced is drastically compromised with respect to the quality of their maturation and integrity, as documented elsewhere (Heasley and McMurray, 2016). Thus, Spr28–Spr3–Cdc3–Cdc10–Cdc10–Cdc3–Spr3–Spr28 complexes have significantly different properties and functions from either Cdc11–Cdc12–Cdc3–Cdc10–Cdc10–Cdc3–Cdc12–Cdc11 or Shs1–Cdc12–Cdc3–Cdc10–Cdc10–Cdc3–Cdc12–Shs1 complexes. Moreover, our FRAP and BiFC analysis indicates that, in vivo, the PSM-associated horseshoes containing the sporulation-specific septins exclude the displaced mitotic septins and are highly organized structures, in agreement with the filaments assembled in vitro on PtdIns4,5P_2-containing monolayers. Thus, sporulation-specific septin complexes, but not mitotic septin complexes, are capable of forming the proper higher-order structures and occupying the correct location to direct efficient spore morphogenesis.

In septin complex formation, guanine nucleotide binding has important roles both in intersubunit contacts at their G interface and for inducing assembly-promoting conformational changes (Sirajuddin et al., 2007, 2009). Moreover, compelling genetic evidence indicates a critical role for GTP binding in yeast septin subunit folding and hetero-octamer assembly in mitotic cells (Weems et al., 2014; Johnson et al., 2015). Crystal structures show that an Asp located in the G-2 motif of the GTP-binding domain in septins and other related small G proteins is important for GTP binding (Wittinghofer and Vetter, 2011). It seems that Spr28 lacks the corresponding Asp residue (Fig. S1 B). In this regard, it is of potential interest that a decrease in intracellular guanine nucleotide production promotes sporulation (Varma et al., 1985). Thus, it is tempting to speculate that, if Spr28 has evolved to no longer require GTP for its folding and assembly, this property and the drop in guanine nucleotide that occurs during meiosis may explain, in part, how formation of sporulation-specific septin complexes outcompetes assembly of residual mitotic septins into complexes.

Yeast sporulation is a form of gametogenesis. As in sporulating yeast, during mammalian spermiogenesis, gamete-specific subunits are incorporated into septin complexes and form higher-order structures distinct from those in mitotically-dividing cells (Lin et al., 2011). SEPT4 is expressed mainly in male germ cells (and postmitotic neural cells) and occupies the same central position in mammalian septin hetero-octamers as Cdc10 does in yeast hetero-octamers (Sandrock et al., 2011). In spermatozoa, SEPT4 is located in the annulus, a cortical ring that separates the middle and principal pieces of a mature sperm from its tail (Kwitny et al., 2010). Nullizygous *sept4*$^{-/-}$ male mice lack a normal annulus and are sterile because of defective sperm morphology and loss of motility of the flagellum (Ihara et al., 2005). SEPT12 is a testis-specific septin that occupies the same terminal position in human septin hetero-octamers as Spr28 does in the sporulation-specific yeast hetero-octamer. Mutations in SEPT12 cause infertility in men (Kuo et al., 2012), demonstrating the functional importance of gametogenesis-specific septins. However, nothing is yet known about the mechanisms involved in "remodeling" the septin repertoire during this (or any other) human cellular differentiation process.

Thus, the molecular organization and properties of the yeast sporulation-specific septin complexes, and the nature of their meiosis-specific interaction partners, will continue to be important models for understanding the unique roles of differentiation-specific septins. Hence, further study of the contributions of individual septin subunits and their development-specific posttranslation modifications in meiosis and other developmental processes in *S. cerevisiae* (e.g., pheromone response and filamentous growth) may shed additional light on general mechanisms that regulate the composition and function of septin complexes in diverse cell types, especially in organisms that, like humans, possess a large number of septin subunits.

Materials and methods

Expression and purification of septin complexes

In general, both the strategy for inducible heterologous expression in *Escherichia coli* and the purification procedure (metal ion affinity, size-exclusion chromatography, and anion exchange] to prepare yeast septin complexes, are described in detail elsewhere (Versele et al., 2004; Bertin et al., 2008; Garcia et al., 2011; Booth et al., 2015). Ligation-independent cloning (Aslanidis and de Jong, 1990) was used to incorporate *CDC3*, *CDC10*, *SPR3*, and/or *SPR28* into bicistronic DUET (Invitrogen) vectors with compatible replication origins, and the resulting plasmids were introduced by DNA-mediated transformation into *E. coli* strain BL1(DE3). The desired transformants were selected on agar plates of Luria–Bertani broth; Bertani, 1951; Luria and Burrous, 1957; Miller, 1972) containing appropriate antibiotics for marker selection (40 µg/ml ampicillin, 34 µg/ml chloramphenicol, and 40 µg/ml kanamycin). Liquid cultures of Luria–Bertani broth containing antibiotics (20 µg/ml ampicillin, 17 µg/ml chloramphenicol, and 20 µg/ml kanamycin) to maintain selection were typically seeded with ∼10 colonies picked directly from the plates and grown overnight at 37°C. We have found that inoculation with multiple colonies yields greater reproducibility in final protein yield and quality from preparation to preparation. Samples (5 ml) of such overnight cultures were, in turn, used to inoculate larger (1 liter) cultures of Tartof–Hobbs medium ("Terrific broth"; Tartof and Hobbs, 1987) with the same antibiotics to maintain selection, which were grown at 37°C to a density of $A_{595\ nm}$ = 0.7, whereupon expression was induced by addition of isopropyl-β-D-thiogalactoside (IPTG; 0.1 mM final concentration) and the culture shifted to 16°C. After 16 h, the cells were harvested by centrifugation at 3,000 *g* and the resulting pellet was resuspended in 10 ml of lysis buffer (40 µM GDP, 12% glycerol, 0.5% Tween-20, 300 mM KCl, 2 mM $MgCl_2$, 20 mM imidazole, and 50 mM Tris-HCl, pH 8.0), flash-frozen by drop-wise addition of the cell resuspension in liquid N_2, and stored at −80°C before use.

Frozen cell pellets were thawed in an ice-water bath, resuspended in lysis buffer-PLUS (5 ml; lysis buffer-PLUS was prepared just before use by adding 10 µl 1-thioglycerol, 40 µl Hercules endonuclease [Genscript], 800 µg lysozyme, and four Halt EDTA-free protease inhibitor tablets [Pierce/Thermo Scientific] to 25 ml of lysis buffer), incubated at 4°C with gentle agitation for 30 min, and then ruptured by four 30-s bursts of sonic irradiation (separated by 2-min periods on ice between

each pulse) at a power output of 6 W. The crude lysate was clarified by centrifugation at 25,000 *g*, and the resulting crude extract was applied using a peristaltic pump to a bed (5 ml) of prepacked Ni^{2+}-charged affinity resin (HisTrap HP; GE Healthcare) at a flow rate of 2 ml/min. After washing with 75 ml wash buffer (25 mM imidazole, 0.1% 1-thioglycerol, 300 mM KCl, and 50 mM Tris-HCL, pH 8.0) at a flow rate of 4 ml/min, bound protein was eluted with 30 ml elution buffer (500 mM imidazole, 0.1% 1-thioglycerol, 300 mM KCl, and 50 mM Tris-HCl, pH 8.0) at a flow rate of 1 ml/min and collected as 1-ml fractions. Protein content of the resulting fractions was assessed using the dye-binding method of Bradford (1976). Fractions with the highest content of septin protein were pooled (6 ml total) and passed through a PVDF membrane (0.2 µm) to remove any particulate material, and the resulting filtrate (5 ml) was loaded onto the top of a bed (in a 120-ml column) of prep-grade Hi-load 16/60 Superdex 200 (GE Healthcare) and eluted with 300 mM KCl, 0.1% 1-thioglycerol, and 50 mM Tris-HCl, pH 8.0, at a flow rate of 0.6 ml/min. In most cases, these two steps were sufficient to yield a purity of ≥90%. If not, the pooled peak fractions from size-exclusion chromatography (determined by $A_{280\ nm}$) were applied to a 1-ml Resource Q column (GE Healthcare) and eluted with a linear salt gradient from 10 mM KCl, 0.1% 1-thioglycerol, 50 mM Tris-HCl, pH 8.0, to 1 M KCl, 0.1% 1-thioglycerol, and 50 mM Tris-HCl, pH 8.0. Aliquots of the peak fractions (as determined by $A_{280\ nm}$) were flash-frozen in liquid N_2 and stored at −80°C until used for experiments.

Analytical size-exclusion chromatography

A septin complex (150 pmol) of interest was loaded onto a Superose 6 PC column, eluted with buffer (75 mM KCl, 2 mM $MgCl_2$, 0.1% 1-thioglycerol, and 50 mM Tris-HCl, pH 8.0) at a flow rate of 0.04 ml/min, and the resulting profile analyzed using an Ettan LC apparatus (GE Healthcare).

Electron microscopy and image processing

Purified septin complexes were diluted to 0.01 mg/ml in either high-salt buffer (300 mM NaCl, 2 mM $MgCl_2$, and 50 mM Tris-HCl, pH 8.0) or low-salt buffer (10 mM NaCl, 2 mM $MgCl_2$, and 50 mM Tris-HCl, pH 8.0) and applied to the surface of a carbon-coated copper EM grid prepared by glow-discharge using an Auto 306 Thermal Evaporator (Edwards). The grids were then washed with water and stained with 2% uranyl formate. Electron micrographs of the adsorbed protein were taken using a Tecnai T12 electron microscope (FEI) operated at 120 kV. Unless otherwise indicated, micrographs were taken at 30,000 magnification and at −1 µm defocus. Data were collected using Leginon (Potter et al., 1999) with a 4k × 4k complementary metal oxide semi-conductor (CMOS) camera (TVIPS TemCam F416). Images of individual complexes (particles) were windowed out of the images with a box size of 135 by 135 pixels using the Boxer program within the EMAN software package (Ludtke et al., 1999). Particles were then aligned and classified using SPIDER (Frank et al., 1996) within the Appion pipeline (Lander et al., 2009). The first round of alignment and classification was reference-free, and class averages representative of the full diversity in length and curvature of the particles in the sample were obtained. These class averages were used as references in subsequent iterations of alignment and classification. After each round, new references were chosen from the class averages produced, and Iterations of alignment and classification were continued until the class averages did not change from one round to the next. Typically, three iterations were performed.

Septin assembly on lipid monolayers

Association of purified recombinant septin complexes with lipid monolayers were performed by slight modifications of prior methods (Kubalek et al., 1991; Taylor et al., 2007; Bertin et al., 2010). In brief, protein samples (20 µl; 100 nM) in low-salt buffer (50 mM KCl and 20 mM Tris-HCl, pH 8.0) were dispensed into polytetrafluoroethylene (Teflon) wells (20 µl), yielding a convex meniscus at the surface. A stock solution (10 mg/ml) of DOPC in chloroform (Avanti Polar Lipids) was diluted to 0.25 mg/ml on the day of use. Stock solutions (1 mg/ml) of either PtdIns4,5P_2 in 9:1::chloroform:methanol (vol/vol; Avanti Polar Lipids) or PtdIns4P in 9:1::chloroform:methanol (vol/vol; Avanti Polar Lipids) were mixed with the DOPC stock solution such that the final phosphoinositide concentration was 15.2 mol% and then diluted to 0.25 mg/ml on the day of use. The desired lipid solution (0.5 µl) was gently spread onto the surface of the protein-containing solution in the Teflon well, which caused a slight flattening of the meniscus. After incubation for 15 h at 4°C in a humidified chamber, the carbon-coated side of a C-flat grid (Proto-chips) with 1.2-µm holes was carefully placed on the surface of the well for 45 s, allowing the lipid monolayer (and any protein associated with its opposite face) to adsorb to the carbon surface. The grids then were lifted vertically from the wells and immediately stained with 2% uranyl formate, air-dried, and viewed by EM as described in the previous section. Micrographs were cropped for publication using ImageJ (National Institutes of Health).

Yeast strains and strain constructions

All yeast strains (Table 1) are derived from BY4741 or BY4742 (Brachmann et al., 1998) and were cultivated and manipulated using standard methods (Amberg et al., 2005). For some experiments, rich ("YP") medium contained tryptone instead of peptone, which had no noticeable effect on growth. BY4742 *sum1Δ0::kanMX* was purchased from Thermo Fisher Scientific. Strain YMVB1 *cdc12(T48N)* (Versele and Thorner, 2004) was crossed with BY4742 *sum1Δ0::kanMX* and, after sporulation, tetrads were dissected to obtain *cdc12(T48N) sum1Δ* haploid. To create a *cdc12-6* derivative of BY4741, the *cdc12-6* allele was first introduced into a *CDC12-GFP* gene on a *HIS3*-marked *CEN* plasmid (pLP29; Lippincott and Li, 1998) by digestion with BfuAI and cotransformation of the cut plasmid into YMVB61 (*cdc12Δ::kanMX* [*CDC12 URA3*]; McMurray et al., 2011) along with *cdc12-6* DNA PCR-amplified from strain DDY1462 (gift of D. Drubin, University of California, Berkeley, Berkeley, CA). Transformants were plated on 5-FOA medium (Boeke et al., 1987), and plasmids were recovered from those colonies that displayed temperature-sensitive growth by rescue in *E. coli* and sequenced to confirm the presence of the *cdc12-6* allele (K391N L392stop). The *CDC12* ORF (including an out-of-frame GFP coding sequence and downstream *HIS3* marker) from one such plasmid (designated YCpH-Cdc12-6) was PCR-amplified and used to transform BY4741, creating the *cdc12-6* mutant used here (MMY0000). JTY3993 (BY4742 *CDC10-mCherry::kanMX*; McMurray et al., 2011) was transformed with BamHI–cut pSC193 (Chu et al., 1998), integrating at the *NDT80* locus a *URA3*-marked copy of *NDT80-HA* behind the *GAL1/10* promoter, creating strain JTY5200. Derivatives of BY4741 carrying *cdc10-1::kanMX* allele (encoding a D182N mutant of Cdc10) and the *cdc12-1::kanMX* allele (encoding a G247E mutant of Cdc12) were obtained from a collection of temperature-sensitive mutants (Li et al., 2011), verified by sequencing the relevant septin gene, and mated with JTY5200 to obtain by subsequent sporulation and tetrad dissection the *cdc10-1* P_{GAL}*-NDT80* strain (MMY0046) and the *cdc12-1* P_{GAL}*-NDT80* strain (MMY0047). A P_{GAL}*-NDT80* derivative of BY4741 with untagged Cdc10 (MMY0048) was created using pSC193, in a similar manner.

To construct yeast strains expressing fluorescently-tagged Spr3 or Spr28 (or both) during vegetative growth, a plasmid-derived DNA fragment encoding the sporulation-specific septin was integrated in place of the endogenous locus for a mitotic septin subunit (*CDC12*

Table 1. **Yeast strains used in this study**

Strain	Genotype	Reference
SF838-1Dα	*MATα ura3-52 leu2-3,112 HIS4 ade6 pep4-3 gal2*	Rothman and Stevens, 1986
DDY1462	*MATα ura3-52 cdc12-6*	Originally from P. Novick, University of California, San Diego, La Jolla, CA
YMVB1	BY4741; *cdc12(T48N)::URA3*	Versele and Thorner, 2004
YMVB61	BY4741; *cdc12Δ::KanR* + pMVB39	McMurray et al., 2011
BY4741	*MAT**a** his3Δ leu2Δ ura3Δ met15Δ*	Brachmann et al., 1998
BY4742	*MATα his3Δ leu2Δ ura3Δ lys2Δ*	Brachmann et al., 1998
BY4743	*MAT**a**/MATα his3Δ/his3Δ leu2Δ/leu2Δ ura3Δ/ura3Δ LYS2/lys2Δ MET15/met15Δ*	Brachmann et al., 1998
JTY5167	BY4742 *sum1Δ::Kan^R*	Genome Deletion Collection
JTY3993	BY4742 *CDC10-mCherry::Kan^R*	McMurray et al., 2011
CBY06417[a]	BY4741 *cdc10-1::Kan^R*	Li et al., 2011
CBY05110[a]	BY4741 *cdc12-1::Kan^R*	Li et al., 2011
GCFY1	BY4742 *cdc11Δ::Kan^R* + pSB1	This study
GCFY2	BY4742 *cdc11Δ::SPR28-GFP-ADH1(t)-Hyg^R* [pJT1520]	This study
GCFY3	BY4741 *cdc12Δ::SPR3-mCherry-ADH1(t)-Kan^R* [pJT1622]	This study
GCFY4	BY4741 *cdc12Δ::SPR3-GFP-ADH1(t)-Hyg^R* [pJT1622]	This study
GCFY5[b]	*MATα cdc11Δ::SPR28-GFP-ADH1(t)-Hyg^R cdc12Δ::SPR3-mCherry-ADH1(t)-Kan^R* [pGCF1/pGCF2]	This study
GCFY6[b]	*MAT**a** cdc11Δ::SPR28-mCherry-ADH1(t)-Kan^R cdc12Δ::SPR3-GFP-ADH1(t)-Hyg^R* [pGCF1/pGCF2]	This study
JTY5168[c]	*sum1Δ::Kan^R cdc12(T48N)::URA3*	This study
MMY0000[d]	BY4741 *cdc12-6::HIS3*	This study
JTY5200[e]	JTY3993 *prGAL1/10-NDT80-HA::URA3*	This study
MMY0046[f]	*cdc10-1::Kan^R prGAL1/10-NDT80-HA::URA3*	This study
MMY0047[g]	*cdc12-1::Kan^R prGAL1/10-NDT80-HA::URA3*	This study
MMY0048[h]	BY4741 *prGAL1/10-NDT80-HA::URA3*	This study
MMY0219	BY4741 *spr3Δ::Kan^R*	Genome Deletion Collection
MMY0220	BY4742 *spr3Δ::Kan^R*	Genome Deletion Collection
MMY0221	BY4743 *spr3Δ::Kan^R/spr3Δ::Kan^R*	This study
MMY0152	BY4741 *spr28Δ::Kan^R*	Genome Deletion Collection
MMY0153	BY4742 *spr28Δ::Kan^R*	Genome Deletion Collection
MMY0154	BY4743 *spr28Δ::Kan^R/spr28Δ::Kan^R*	This study
MMY0231	BY4743 *spr3Δ::Kan^R/spr3Δ::Kan^R spr28Δ::Kan^R/spr28Δ::Kan^R*	This study
GCFY7	BY4743 *spr28Δ::CDC11*::eGFP::*Nat^R* / *spr28Δ::CDC11*::eGFP::*Hyg^R spr3Δ::CDC12*::mCherry::*Kan^R* / *spr3Δ::CDC12*::mCherry::*Kan^R*	This study
FY2742	*MATα his3Δ1 leu2Δ0 lys2Δ0 ura3Δ0 MKT1(G30) RME1 TAO3(Q1493)*	F. Winston, Harvard Medical School, Boston, MA
FY2839	*MAT**a** his3Δ1 leu2Δ0 lys2Δ0 ura3Δ0 MKT1(G30) RME1 TAO3(Q1493)*	F. Winston
MMY0185	FY2839 *spr3Δ::Kan^R*	This study
MMY0222	FY2742 *spr3Δ::Kan^R*	This study
MMY0186	FY2839 *spr28Δ::Kan^R*	This study
MMY0155	FY2742 *spr28Δ::Kan^R*	This study
MMY0149	FY2742 *CDC12-eCitrine::his5MX*	This study
MMY0228	*rme1/RME1 mkt1/MKT1 tao3/TAO3 CDC12/CDC12-eCitrine::his5MX*	This study
MMY0229	FY2742 *spr28Δ::Kan^R CDC12-eCitrine::his5MX*	This study
MMY0230	*rme1/RME1 mkt1/MKT1 tao3/TAO3 spr3Δ::CDC12/SPR3$^+$ spr28Δ::CDC11/SPR28$^+$ CDC12/CDC12-eCitrine::his5MX*	This study
MMY0226	*rme1/RME1 mkt1/MKT1 tao1/TAO1 SPR28/spr28Δ::SHS1*::Vc::*HIS3MX6 SPR3/spr3Δ::CDC12*::mCherry::*Kan^R*	This study
YO685	*MATα his3-Δ200 leu2-Δ1 lys2-801 trp1-Δ63 ura3-52 CDC3-Vc::HIS3^{MX6}*	Oh et al., 2013
YEF5690	*MAT**a** his3-Δ200 leu2-Δ1 lys2-801 trp1-Δ63 ura3-52 CDC10-Vn::kan^{MX6}*	Oh et al., 2013
YEF5692	*MAT**a** his3-Δ200 leu2-Δ1 lys2-801 trp1-Δ63 ura3-52 CDC12-Vn::TRP1* [pRS316 *CDC12*]	Oh et al., 2013
MMY0224	BY4742 *SPR3-Vn::URA3*	This study

[a]Sequence analysis of the relevant coding regions from these strains confirmed the mutant alleles to be *cdc10(D182N; cdc10-1)* and *cdc12(G247E; cdc12-1)*.
[b]In both GCFY5 and GCFY6, *SPR28* is under control of the endogenous *CDC11* promoter and *SPR3* is under control of the endogenous *CDC12* promoter, and both GCFY5 and GCFY6 may also harbor the original, *URA3*-marked covering plasmids pSB1/pJT1520 and/or pMVB39/pJT1622. Subsequent strain propagation was performed to select for the presence of either pGCF1 or pGCF2 (or both) for certain experiments.
[c]Spore from cross of YMVB1 with JTY5167.
[d]BY4741 was transformed with a PCR product amplified from YCpH-*cdc12-6* that included the 3′ end of the *cdc12-6* coding sequence, the out-of-frame GFP coding sequence, and downstream *HIS3* marker.
[e]JTY3993 was transformed with BamHI–cut pSC193.
[f]Spore from cross of JTY5200 with CBY06417.
[g]Spore from cross of JTY5200 with CBY05110.
[h]BY4741 was transformed with BamHI-cut pSC193.

or *CDC11*, respectively), as follows. A PCR fragment containing the *CDC11$_{prom}$-SPR28*-GFP-ADH(t)-Hyg^R (treated with DpnI restriction endonuclease to destroy any intact vector) was used to transform a *cdc11Δ::Kan^R* yeast strain (covered by pRS316-*CDC11*), where the *cdc11Δ::Kan^R* allele represents a full deletion of the *CDC11* coding sequence and the drug-resistance cassette is in the same orientation as the ORF, leaving the promoter region and the MX4 cassette terminator, which is identical between the drug-resistance cassettes (Goldstein and McCusker, 1999), to mediate the homologous recombination to achieve integration at the *CDC11* locus. A similar strategy was used to

integrate *CDC12*$_{prom}$-*SPR3*-GFP-ADH(t)-Hyg^R. To create a strain coexpressing both *SPR28* and *SPR3*, the individual strains (one *MAT***a**, the other *MAT*α) were first transformed with differentially marked covering plasmids expressing the corresponding wild-type septin (*CDC11::URA3-HIS3* and *CDC12::URA3-LEU2*, respectively), then mated together. After diploid selection and sporulation, tetrads were dissected and the desired haploid spores were identified by selection for the drug resistance markers diagnostic of the integrated alleles and the covering plasmids and then confirmed by growth phenotype, diagnostic PCR, and immunoblot analysis and fluorescence microscopy.

MMY0231 (*MAT***a**/*MAT*α *spr3Δ/spr3Δ spr28Δ/spr28Δ*) was created by mating appropriate spore clones isolated from a cross of MMY0220 and MMY0152 (Table 1). To generate strain GCFY7, which lacks Spr28 and Spr3 and expresses in their place (and in a meiosis-specific manner) both Cdc11 and Cdc12, respectively, the *SPR28* locus was deleted in BY4742, yielding GFY-853 (*MAT*α *spr28Δ::Kan^R*), followed by deletion of the *SPR3* locus producing GFY-885 (*MAT*α *spr28Δ::Kan^R spr3ΔHyg^R*). Next, plasmids were constructed that express *CDC11-GFP::Nat^R* (pGF-IVL291) and *CDC12-mCherry*::*Kan^R* (pGF-IVL295) under control of the *SPR28* and *SPR3* promoters, respectively, using in vivo ligation and homologous recombination (Finnigan and Thorner, 2015). After PCR amplification with appropriate primers containing the necessary regions of homology and DpnI treatment, the *CDC11*-GFP-containing PCR product was integrated at the *SPR28* locus (to generate strain GFY-920) and the *CDC12*-mCherry-containing PCR product was integrated at the *SPR3* locus (creating strain GFY-983). Then, a *URA3*-based Gal-inducible *HO*-expressing plasmid (pJT2800) was introduced into GFY-983 to generate a derivative in which the mating type was switched from *MAT*α to *MAT***a** (and the plasmid was removed by selection on medium containing 5-FOA), yielding GFY-1041. Lastly, the Nat^R marker at the *SPR28* locus in GFY-983 was swapped to Hyg^R, generating strain GFY-1030. Multiple diagnostic PCR reactions and nucleotide sequence analysis confirmed proper integration at each modified locus, as well as *MAT* identity. Finally, GCFY7 was created by (1) mating GFY-1030 with GFY-1041 on YPD medium for 24 h at 30°C and (2) two successive growth selections for clonal diploid isolates on rich medium containing both Nourseothricin (clonNat) and Hygromycin. BY4743 *spr3Δ::kanMX/spr3Δ::kanMX* and BY4743 *spr28Δ::kanMX/spr28Δ::kanMX* strains were constructed by first recreating the haploid deletion strains in BY4741 and BY4742, via transformations of those strains with PCR products that amplified the *spr3Δ::kanMX* or *spr28Δ::kanMX* cassette, including several hundred base pairs upstream and downstream of the former *SPR* gene ORF. These haploid mutants were then mated together to form the homozygous diploid strains. The same haploid transformation method was used to introduce the deletion alleles into strains carrying the SK1 alleles at *TAO3*, *MKT1*, and *RME1*. To make strain MMY0225, a PCR product made with a primer annealing to the 5′ region of the *SHS1* ORF and including 40 nt upstream of the *SPR28* ORF was used with an appropriate reverse primer including 40 nt downstream of the *SPR28* stop codon to amplify *SHS1-V$_C$::HIS3MX6* from genomic DNA of Y0619, and this product was transformed into GFY-983. This strain was mated with FY2839 to create MMY0226. To integrate CDC12-eCitrine, PCR was used to amplify the *CDC12-eCitrine::his5MX* cassette from plasmid pML113, and the DpnI-digested product was transformed into the appropriate strain.

Plasmids and their construction

Plasmids (Table 2) expressing fluorescently tagged Spr28 and Spr3 under control of the endogenous *CDC11* and *CDC12* promoters were constructed by in vivo ligation and homologous recombination (Muhlrad et al., 1992; Finnigan and Thorner, 2015) in strain SF838-1Da (Rothman and Stevens, 1986), as follows. Plasmid pRS315 containing 500 bp of the *CDC11* promoter was gapped and cotransformed into yeast with PCR-generated linear DNA fragments containing full-length *SPR28* ORF and the GFP-ADH1(t)-Hyg^R cassette (Goldstein and McCusker, 1999), each with corresponding 30-bp homologous tails. A similar procedure was used to create the *SPR3*-mCherry–expressing vector. To create vectors containing wild-type *CDC11* or *CDC12* that were differentially marked (in addition to containing *URA3* for counterselection on 5-FOA), the same in vivo ligation approach was used to create pRS313-*CDC11*-ADH1(t)-*CaURA3* and pRS315-*CDC12*-ADH1(t)-*CaURA3*. Constructs were recovered from yeast by rescue in *E. coli* and confirmed via diagnostic PCR and DNA sequencing.

Assessment of yeast growth rates and morphologies

In a 96-well plate, eight 100-µl cultures of each of six yeast strains were grown in YP containing 2% raffinose (“YPRaf”) or 2% raffinose

Table 2. **Plasmids used in this study**

Plasmid	Description	Reference
pRS315	*CEN, LEU2*	Sikorski and Hieter, 1989
pRS313	*CEN, HIS3*	Sikorski and Hieter, 1989
pLP29	*pRS313; CDC12-GFP*	Lippincott and Li, 1998
pSB1 / pJT1520	*CEN, URA3, CDC11*	Versele et al., 2004
pMVB39 / pJT1622	*CEN, URA3, CDC12*	Versele and Thorner, 2004
pSC193	*URA3, prGAL1/10-NDT80-HA*	Chu and Herskowitz, 1993
YCpH-*cdc12-6*[a]	*pLP29; cdc12-6*	This study
pGCF1	pRS313; *prCDC11-CDC11-ADH1(t)-CaURA3*	This study
pGCF2	pRS315; *prCDC12-CDC12-ADH1(t)-SpHIS5*	This study
pGCF3	pRS315; *prCDC11-SPR28-GFP-ADH1(t)-Hyg^R*	This study
pGCF4	pRS313; *prCDC12-SPR3-mCherry-ADH1(t)-Kan^R*	This study
p3.8	*CDC3, CDC10, His$_6$-SPR3* in *E. coli*	This study
p4.7	*CDC3, CDC10, His$_6$-SPR3, SPR28* in *E. coli*	This study
p4.10	*CDC3, CDC10, His$_6$-SPR3, CDC11* in *E. coli*	This study
pJT2485	p406-GFP-2XPH^{Osh2}	Roy and Levine, 2004
pML113	*CEN, LEU2, CDC12-eCitrine::his5MX*	Nagaraj et al., 2008

[a]The *cdc12-6* allele was first introduced into a *CDC12-GFP* gene on pLP29 by digestion with *Bfu*AI and co-transformation of the cut plasmid into YMVB61 along with the PCR-amplified *cdc12-6* gene from DDY1462. Plasmids from transformants that displayed temperature sensitivity upon loss of the *URA3*-marked *CDC12* plasmid were rescued to *E. coli* and sequenced to confirm the presence of the *cdc12-6* allele (K391N L392stop).

plus 0.05% galactose ("YPRafGal") at 25.4°C inside a BioTek Synergy HT plate reader, and $A_{630\ nm}$ was measured every 10 min over 15 h (in between reads, the plate was agitated on the medium setting). Growth rates and associated standard errors were calculated using Prism 5.0d (GraphPad Software). Cells from these cultures, or from agar plates, were resuspended in H_2O and examined at 22°C by transmitted light using an EVOSfl microscope (Advanced Microscopy Group) equipped with a monochrome charge-coupled device (ICX285AL; Sony), 2/3" 1,360 × 1,024, 1.4-Megapixel camera and an Olympus 60× PlanApo 1.42 NA objective and categorized. Images were captured using the software built into the microscope, and cropped and contrast-adjusted using Adobe Photoshop. In other experiments, yeast cultures were grown overnight in synthetic medium with 2% glucose with selection for covering plasmids; for cells coexpressing both Spr28 and Spr3, selection for the vectors containing the wild-type copies of *CDC11* and *CDC12* was used. In complementation tests, fivefold serial dilutions of the strains were spotted on solid synthetic-complete medium with 2% glucose lacking or containing 5-FOA, and scored after incubation at 30°C for 2–3 d.

Fluorescence microscopy and imaging

Yeast were grown overnight in synthetic medium selective for covering plasmid(s), diluted to an $A_{600\ nm}$ of 0.25/ml in YPD medium, and grown for 4–4.5 h (until $A_{600\ nm}$ was ∼1). The resulting cells were harvested, washed with water, and examined using a BH-2 epifluorescence microscope (Olympus) under a 100× objective. Images were obtained using a charge-coupled device camera (Olympus), Magnafire SP software (Optronics), and Adobe Photoshop. To quantify the fraction of cells with septin localization at the bud neck, images of cells (n = 100–250) for two technical replicates from at least three independent trials were scored (error represents the standard deviation of the mean of these measurements). Images of control cells (n = 50–100) expressing GFP fused to the C termini of Cdc11 or Cdc12 were also scored; similar images and quantification were obtained mCherry was used in place of GFP. Cells that displayed an extreme elongated morphology (caused by loss of the wild-type septin) were excluded from the analysis. For the strain expressing both Spr28-GFP and Spr3-mCherry, only cells displaying detectible GFP signal were scored.

Preparation of cell extracts and immunoblotting

Yeast strains were grown overnight in selective medium, diluted to an $A_{600\ nm}$ = 0.25/ml in fresh medium and grown to $A_{600\ nm}$ ∼1. Cells from samples (2 ml) of the cultures were harvested and frozen at −80°C. The frozen cells were resuspended and lysed in 1.85 M NaOH and 7.4% 2-mercaptoethanol (2-ME) and protein was precipitated using 50% trichloroacetic acid on ice for 10 min. After washing the resulting precipitates in acetone, protein was solubilized in 5% SDS and 0.1 M Tris, followed by addition of 0.2 volumes of a 5× stock of SDS gel sample buffer (10% SDS, 50% glycerol, 7.5 mM bromophenol blue, 0.715 M 2-ME, and 0.25 M Tris, pH 6.8). After boiling and clarification by brief centrifugation in a microfuge, samples (12 µl) were resolved by SDS-PAGE, transferred to nitrocellulose, probed with rabbit polyclonal anti-Pgk1 (Baum et al., 1978), mouse monoclonal anti-GFP (Roche Applied Sciences), or rabbit polyclonal anti-DsRed (Rockland) primary antibodies and appropriate infrared dye-conjugated secondary antibodies (Li-Cor) and visualized using an Odyssey infrared imaging device (Li-Cor).

Assessment of sporulation proficiency

The cells in triplicate samples (250 µl) of liquid cultures of the *MAT***a**/*MAT*α strains to be tested, which had been grown to saturation in rich medium (YPGlc), were collected by centrifugation, washed twice with sterile H_2O, and resuspended in 2 ml sporulation medium (1% potassium acetate, 0.05% glucose, 20 mg/ml leucine, and 40 mg/ml uracil). The resulting cell suspensions were incubated at room temperature (∼22°C) with gentle aeration on a rollerdrum and then examined after ∼5 d. A total of at least 300 individual cells were scored per sample; values obtained for any given genotype were averaged for at least three-to-six independent trials. Mature spores were identified as bright spheres of ≤5 µm diameter because completed spore walls refract the illuminating light when viewed by standard transmission microscopy. This method for scoring sporulation efficiency was validated by two independent means: (1) introducing into the strains tested a plasmid expressing a fluorescently tagged histone, Htb2-mCherry (Westfall et al., 2008), to accentuate the number of nuclear lobes present at meiosis II; and (2) introducing into the strains tested a plasmid expressing a fluorescently tagged exo–β-glucanase, Spr1-GFP (Suda et al., 2009), that specifically decorates the wall of mature spores (Heasley and McMurray, 2016). The differences between the sporulation efficiency (% asci) of the wild-type controls and the other strains examined were statistically significant to better than the 95% confidence level based on the standard one-tailed Fisher's exact test.

FRAP

FRAP was performed as previously described (Maddox et al., 2000; Molk et al., 2004). In brief, cells expressing either *CDC10*-GFP or GFP-2X(PH^{Osh2}) were imaged at 25°C using an inverted TiE microscope (Nikon) equipped with a Xyla CMOS camera (Andor) and a 100× PlanApo 1.4 NA objective. Photobleaching was performed using a Coherent 488 nm Sapphire 50-mW laser through an LU4A laser module (Nikon) controlled by Nikon Elements software. Three prebleach images (600-ms exposure) were acquired to establish a baseline control for the initial fluorescence. A single focused 50-ms laser pulse was used to photobleach a Cdc10-GFP–containing horseshoe in sporulating cells (or, for GFP-2X(PH^{Osh2}), a well-decorated portion of the PSM). The photobleaching treatment eliminated 75–95% of the original fluorescence. Immediately thereafter, single plane images (600-ms exposures) were acquired every 10 s for ∼2 min to follow any recovery. Such photobleaching experiments were performed on 15 different cells. Using ImageJ analysis software (National Institutes of Health), the observed fluorescence intensity values were corrected for background and photobleaching during image acquisition and displayed as the mean relative value for the bleached and unbleached regions for all 15 cells.

Bimolecular fluorescence complementation

*MAT***a**/*MAT*α diploids containing the proteins of interest fused to the two nonfluorescent halves of the Venus derivative (F46L F64L M153T V163A S175G; Rekas et al., 2002) of the YFP variant of GFP (Griesbeck et al., 2001) were made by mating the appropriate haploid strains, the majority of which were generously provided by E. Bi (University of Pennsylvania, Philadelphia, PA). The diploids were induced to sporulate as described in the Assessment of sporulation proficiency section and spotted in water directly from the sporulation cultures onto "pads" of 2% agarose, and any resulting yellow fluorescence arising from the reconstitution of the chromophore upon association of the interacting proteins (Kerppola, 2008) was imaged at 22°C using the EVOSfl microscope and 60× objective with a YFP filter cube (excitation, 500 nm; emission, 542 nm). Images were captured using the software built into the microscope and cropped and contrast-adjusted using Photoshop and/or ImageJ.

Online supplemental material

Table S1 catalogs the sequence relatedness among all seven *S. cerevisiae* septins. Fig. S1 depicts sequence features of the sporulation-specific

septins. Fig. S2 shows that switching fluorescent tags on Spr3 and Spr28 does not alter their corecruitment to the bud neck in vegetative cells. Fig. S3 shows that ectopic expression of *SPR3* and/or *SPR28* does not impede the growth of wild-type mitotic cells. Fig. S4 shows that ectopic expression of sporulation-specific septins does exacerbate the growth defects of mitotic cells carrying mutations in mitosis-specific septins. Fig. S5 shows that expression of sporulation-specific septins driven by low-level ectopic expression of transcription factor Ndt80 in a *cdc12-1* mutant causes an increased frequency of mitotic cells with an aberrant morphology. Online supplemental material is available at http://www.jcb.org/cgi/content/full/jcb.201511029/DC1.

Acknowledgments

We thank A. Neiman, M. Onishi, and J. Pringle for helpful discussions and the communication of unpublished results; A. Vershon for providing the *NDT80* plasmid; E. Bi and Fred Winston for the generous gift of strains; and the QB3 MacroLab (University of California, Berkeley), established with and supported by funds provided by the W.M. Keck Foundation, for help preparing some of the constructs used for expression and purification of the sporulation-specific septins.

This work was supported by a National Science Foundation predoctoral fellowship (to G. Garcia III), a postdoctoral fellowship from the Adolph C. and Mary Sprague Miller Institute for Basic Research in Science, University of California Berkeley (to G.C. Finnigan), a National Institutes of Health Predoctoral Traineeship GM008730 (to L.R. Heasley), a National Institutes of Health R01 research grant GM099820 (to C.G. Pearson), a National Institutes of Health K99/R00 Pathway to Independence Award GM086603 (to M.A. McMurray), and a National Institutes of Health R01 research grant GM101314 (to E. Nogales and J. Thorner). E. Nogales is a Howard Hughes Medical Institute Investigator.

The authors declare no competing financial interests.

Submitted: 8 November 2015
Accepted: 22 January 2016

References

Amberg, D.C., D.J. Burke, and J.N. Strathern. 2005. Methods in Yeast Genetics: A Cold Spring Harbor Laboratory Course Manual. Cold Spring Harbor Laboratory Press, Cold Spring Harbor, NY. 230 pp.

An, H., J.L. Morrell, J.L. Jennings, A.J. Link, and K.L. Gould. 2004. Requirements of fission yeast septins for complex formation, localization, and function. *Mol. Biol. Cell.* 15:5551–5564. http://dx.doi.org/10.1091/mbc.E04-07-0640

Aslanidis, C., and P.J. de Jong. 1990. Ligation-independent cloning of PCR products (LIC-PCR). *Nucleic Acids Res.* 18:6069–6074. http://dx.doi.org/10.1093/nar/18.20.6069

Baum, P., J. Thorner, and L. Honig. 1978. Identification of tubulin from the yeast Saccharomyces cerevisiae. *Proc. Natl. Acad. Sci. USA*. 75:4962–4966. http://dx.doi.org/10.1073/pnas.75.10.4962

Bertani, G. 1951. Studies on lysogenesis. I. The mode of phage liberation by lysogenic Escherichia coli. *J. Bacteriol.* 62:293–300.

Bertin, A., M.A. McMurray, P. Grob, S.S. Park, G. Garcia III, I. Patanwala, H.L. Ng, T. Alber, J. Thorner, and E. Nogales. 2008. *Saccharomyces cerevisiae* septins: supramolecular organization of heterooligomers and the mechanism of filament assembly. *Proc. Natl. Acad. Sci. USA.* 105:8274–8279. http://dx.doi.org/10.1073/pnas.0803330105

Bertin, A., M.A. McMurray, L. Thai, G. Garcia III, V. Votin, P. Grob, T. Allyn, J. Thorner, and E. Nogales. 2010. Phosphatidylinositol-4,5-bisphosphate promotes budding yeast septin filament assembly and organization. *J. Mol. Biol.* 404:711–731. http://dx.doi.org/10.1016/j.jmb.2010.10.002

Boeke, J.D., J. Trueheart, G. Natsoulis, and G.R. Fink. 1987. 5-Fluoroorotic acid as a selective agent in yeast molecular genetics. *Methods Enzymol.* 154:164–175. http://dx.doi.org/10.1016/0076-6879(87)54076-9

Booth, E.A., E.W. Vane, D. Dovala, and J. Thorner. 2015. A Förster resonance energy transfer (FRET)-based system provides insight into the ordered assembly of yeast septin hetero-octamers. *J. Biol. Chem.* 290:28388–28401. http://dx.doi.org/10.1074/jbc.M115.683128

Börner, G.V., and R.S. Cha. 2015. Induction and analysis of synchronous meiotic yeast cultures. *Cold Spring Harb. Protoc.* 2015:908–913. http://dx.doi.org/10.1101/pdb.prot085035

Brachmann, C.B., A. Davies, G.J. Cost, E. Caputo, J. Li, P. Hieter, and J.D. Boeke. 1998. Designer deletion strains derived from Saccharomyces cerevisiae S288C: a useful set of strains and plasmids for PCR-mediated gene disruption and other applications. *Yeast.* 14:115–132. http://dx.doi.org/10.1002/(SICI)1097-0061(19980130)14:2<115::AID-YEA204>3.0.CO;2-2

Bradford, M.M. 1976. A rapid and sensitive method for the quantitation of microgram quantities of protein utilizing the principle of protein-dye binding. *Anal. Biochem.* 72:248–254. http://dx.doi.org/10.1016/0003-2697(76)90527-3

Brar, G.A., M. Yassour, N. Friedman, A. Regev, N.T. Ingolia, and J.S. Weissman. 2012. High-resolution view of the yeast meiotic program revealed by ribosome profiling. *Science.* 335:552–557. http://dx.doi.org/10.1126/science.1215110

Caviston, J.P., M. Longtine, J.R. Pringle, and E. Bi. 2003. The role of Cdc42p GTPase-activating proteins in assembly of the septin ring in yeast. *Mol. Biol. Cell.* 14:4051–4066. http://dx.doi.org/10.1091/mbc.E03-04-0247

Chu, S., J. DeRisi, M. Eisen, J. Mulholland, D. Botstein, P.O. Brown, and I. Herskowitz. 1998. The transcriptional program of sporulation in budding yeast. *Science.* 282:699–705. http://dx.doi.org/10.1126/science.282.5389.699

de Almeida Marques, I., N.F. Valadares, W. Garcia, J.C. Damalio, J.N. Macedo, A.P. de Araújo, C.A. Botello, J.M. Andreu, and R.C. Garratt. 2012. Septin C-terminal domain interactions: implications for filament stability and assembly. *Cell Biochem. Biophys.* 62:317–328. http://dx.doi.org/10.1007/s12013-011-9307-0

De Virgilio, C., D.J. DeMarini, and J.R. Pringle. 1996. *SPR28*, a sixth member of the septin gene family in *Saccharomyces cerevisiae* that is expressed specifically in sporulating cells. *Microbiology.* 142:2897–2905. http://dx.doi.org/10.1099/13500872-142-10-2897

Dobbelaere, J., M.S. Gentry, R.L. Hallberg, and Y. Barral. 2003. Phosphorylation-dependent regulation of septin dynamics during the cell cycle. *Dev. Cell.* 4:345–357. http://dx.doi.org/10.1016/S1534-5807(03)00061-3

Douglas, L.M., F.J. Alvarez, C. McCreary, and J.B. Konopka. 2005. Septin function in yeast model systems and pathogenic fungi. *Eukaryot. Cell.* 4:1503–1512. http://dx.doi.org/10.1128/EC.4.9.1503-1512.2005

Enyenihi, A.H., and W.S. Saunders. 2003. Large-scale functional genomic analysis of sporulation and meiosis in *Saccharomyces cerevisiae. Genetics.* 163:47–54.

Fares, H., L. Goetsch, and J.R. Pringle. 1996. Identification of a developmentally regulated septin and involvement of the septins in spore formation in *Saccharomyces cerevisiae. J. Cell Biol.* 132:399–411. http://dx.doi.org/10.1083/jcb.132.3.399

Finnigan, G.C., and J. Thorner. 2015. Complex *in vivo* ligation using homologous recombination and high-efficiency plasmid rescue from *Saccharomyces cerevisiae. Bio Protoc.* 5:e1521.

Finnigan, G.C., J. Takagi, C. Cho, and J. Thorner. 2015. Comprehensive genetic analysis of paralogous terminal septin subunits Shs1 and Cdc11 in *Saccharomyces cerevisiae. Genetics.* 200:821–841. http://dx.doi.org/10.1534/genetics.115.176495

Fowell, R.R. 1969. Sporulation and hybridization of yeast. *In* The Yeasts. Vol. 1. A.H. Rose, and J.S. Harrison, editors. Academic Press, Inc., New York, NY. 303–383.

Frank, J., M. Radermacher, P. Penczek, J. Zhu, Y. Li, M. Ladjadj, and A. Leith. 1996. SPIDER and WEB: processing and visualization of images in 3D electron microscopy and related fields. *J. Struct. Biol.* 116:190–199. http://dx.doi.org/10.1006/jsbi.1996.0030

Friedlander, G., D. Joseph-Strauss, M. Carmi, D. Zenvirth, G. Simchen, and N. Barkai. 2006. Modulation of the transcription regulatory program in yeast cells committed to sporulation. *Genome Biol.* 7:R20. http://dx.doi.org/10.1186/gb-2006-7-3-r20

Garcia, G. III, A. Bertin, Z. Li, Y. Song, M.A. McMurray, J. Thorner, and E. Nogales. 2011. Subunit-dependent modulation of septin assembly: budding yeast septin Shs1 promotes ring and gauze formation. *J. Cell Biol.* 195:993–1004. http://dx.doi.org/10.1083/jcb.201107123

Goldstein, A.L., and J.H. McCusker. 1999. Three new dominant drug resistance cassettes for gene disruption in *Saccharomyces cerevisiae. Yeast.*

15:1541–1553. http://dx.doi.org/10.1002/(SICI)1097-0061(199910)15:14<1541::AID-YEA476>3.0.CO;2-K

Griesbeck, O., G.S. Baird, R.E. Campbell, D.A. Zacharias, and R.Y. Tsien. 2001. Reducing the environmental sensitivity of yellow fluorescent protein. Mechanism and applications. *J. Biol. Chem.* 276:29188–29194. http://dx.doi.org/10.1074/jbc.M102815200

Heasley, L.R., and M.A. McMurray. 2016. Roles of septins in prospore membrane morphogenesis and spore wall assembly in *S. cerevisiae*. *Mol. Biol. Cell.* http://dx.doi.org/10.1091/mbc.E15-10-0721

Ihara, M., A. Kinoshita, S. Yamada, H. Tanaka, A. Tanigaki, A. Kitano, M. Goto, K. Okubo, H. Nishiyama, O. Ogawa, et al. 2005. Cortical organization by the septin cytoskeleton is essential for structural and mechanical integrity of mammalian spermatozoa. *Dev. Cell.* 8:343–352. http://dx.doi.org/10.1016/j.devcel.2004.12.005

Johnson, C.R., A.D. Weems, J.M. Brewer, J. Thorner, and M.A. McMurray. 2015. Cytosolic chaperones mediate quality control of higher-order septin assembly in budding yeast. *Mol. Biol. Cell.* 26:1323–1344. http://dx.doi.org/10.1091/mbc.E14-11-1531

Kaback, D.B., and L.R. Feldberg. 1985. *Saccharomyces cerevisiae* exhibits a sporulation-specific temporal pattern of transcript accumulation. *Mol. Cell. Biol.* 5:751–761. http://dx.doi.org/10.1128/MCB.5.4.751

Kao, G., D.G. Mannix, B.L. Holaway, M.C. Finn, A.E. Bonny, and M.J. Clancy. 1989. Dependence of inessential late gene expression on early meiotic events in *Saccharomyces cerevisiae*. *Mol. Gen. Genet.* 215:490–500. http://dx.doi.org/10.1007/BF00427048

Kerppola, T.K. 2008. Bimolecular fluorescence complementation (BiFC) analysis as a probe of protein interactions in living cells. *Annu. Rev. Biophys.* 37:465–487. http://dx.doi.org/10.1146/annurev.biophys.37.032807.125842

Kim, M.S., C.D. Froese, M.P. Estey, and W.S. Trimble. 2011. SEPT9 occupies the terminal positions in septin octamers and mediates polymerization-dependent functions in abscission. *J. Cell Biol.* 195:815–826. http://dx.doi.org/10.1083/jcb.201106131

Kim, M.S., C.D. Froese, H. Xie, and W.S. Trimble. 2012. Uncovering principles that control septin-septin interactions. *J. Biol. Chem.* 287:30406–30413. http://dx.doi.org/10.1074/jbc.M112.387464

Kubalek, E.W., R.D. Kornberg, and S.A. Darst. 1991. Improved transfer of two-dimensional crystals from the air/water interface to specimen support grids for high-resolution analysis by electron microscopy. *Ultramicroscopy.* 35:295–304. http://dx.doi.org/10.1016/0304-3991(91)90082-H

Kuo, Y.C., Y.H. Lin, H.I. Chen, Y.Y. Wang, Y.W. Chiou, H.H. Lin, H.A. Pan, C.M. Wu, S.M. Su, C.C. Hsu, and P.L. Kuo. 2012. SEPT12 mutations cause male infertility with defective sperm annulus. *Hum. Mutat.* 33:710–719. http://dx.doi.org/10.1002/humu.22028

Kwitny, S., A.V. Klaus, and G.R. Hunnicutt. 2010. The annulus of the mouse sperm tail is required to establish a membrane diffusion barrier that is engaged during the late steps of spermiogenesis. *Biol. Reprod.* 82:669–678. http://dx.doi.org/10.1095/biolreprod.109.079566

Lander, G.C., S.M. Stagg, N.R. Voss, A. Cheng, D. Fellmann, J. Pulokas, C. Yoshioka, C. Irving, A. Mulder, P.W. Lau, et al. 2009. Appion: an integrated, database-driven pipeline to facilitate EM image processing. *J. Struct. Biol.* 166:95–102. http://dx.doi.org/10.1016/j.jsb.2009.01.002

Li, Z., F.J. Vizeacoumar, S. Bahr, J. Li, J. Warringer, F.S. Vizeacoumar, R. Min, B. Vandersluis, J. Bellay, M. Devit, et al. 2011. Systematic exploration of essential yeast gene function with temperature-sensitive mutants. *Nat. Biotechnol.* 29:361–367. http://dx.doi.org/10.1038/nbt.1832

Lin, Y.H., Y.C. Kuo, H.S. Chiang, and P.L. Kuo. 2011. The role of the septin family in spermiogenesis. *Spermatogenesis.* 1:298–302. http://dx.doi.org/10.4161/spmg.1.4.18326

Lippincott, J., and R. Li. 1998. Sequential assembly of myosin II, an IQGAP-like protein, and filamentous actin to a ring structure involved in budding yeast cytokinesis. *J. Cell Biol.* 140:355–366. http://dx.doi.org/10.1083/jcb.140.2.355

Longtine, M.S., D.J. DeMarini, M.L. Valencik, O.S. Al-Awar, H. Fares, C. De Virgilio, and J.R. Pringle. 1996. The septins: roles in cytokinesis and other processes. *Curr. Opin. Cell Biol.* 8:106–119. http://dx.doi.org/10.1016/S0955-0674(96)80054-8

Ludtke, S.J., P.R. Baldwin, and W. Chiu. 1999. EMAN: semiautomated software for high-resolution single-particle reconstructions. *J. Struct. Biol.* 128:82–97. http://dx.doi.org/10.1006/jsbi.1999.4174

Luria, S.E., and J.W. Burrous. 1957. Hybridization between *Escherichia coli* and *Shigella*. *J. Bacteriol.* 74:461–476.

Maddox, P.S., K.S. Bloom, and E.D. Salmon. 2000. The polarity and dynamics of microtubule assembly in the budding yeast *Saccharomyces cerevisiae*. *Nat. Cell Biol.* 2:36–41. http://dx.doi.org/10.1038/71357

Maier, P., N. Rathfelder, M.G. Finkbeiner, C. Taxis, M. Mazza, S. Le Panse, R. Haguenauer-Tsapis, and M. Knop. 2007. Cytokinesis in yeast meiosis depends on the regulated removal of Ssp1p from the prospore membrane. *EMBO J.* 26:1843–1852. http://dx.doi.org/10.1038/sj.emboj.7601621

McMurray, M.A., and J. Thorner. 2008. Septin stability and recycling during dynamic structural transitions in cell division and development. *Curr. Biol.* 18:1203–1208. http://dx.doi.org/10.1016/j.cub.2008.07.020

McMurray, M.A., and J. Thorner. 2009. Reuse, replace, recycle. Specificity in subunit inheritance and assembly of higher-order septin structures during mitotic and meiotic division in budding yeast. *Cell Cycle.* 8:195–203. http://dx.doi.org/10.4161/cc.8.2.7381

McMurray, M.A., A. Bertin, G. Garcia III, L. Lam, E. Nogales, and J. Thorner. 2011. Septin filament formation is essential in budding yeast. *Dev. Cell.* 20:540–549. http://dx.doi.org/10.1016/j.devcel.2011.02.004

Miller, J.H. 1972. Experiments in Molecular Genetics. Cold Spring Harbor Laboratory Press, Cold Spring Harbor, NY. 466 pp.

Moens, P.B. 1971. Fine structure of ascospore development in the yeast *Saccharomyces cerevisiae*. *Can. J. Microbiol.* 17:507–510. http://dx.doi.org/10.1139/m71-084

Molk, J.N., S.C. Schuyler, J.Y. Liu, J.G. Evans, E.D. Salmon, D. Pellman, and K. Bloom. 2004. The differential roles of budding yeast Tem1p, Cdc15p, and Bub2p protein dynamics in mitotic exit. *Mol. Biol. Cell*. 15:1519–1532. http://dx.doi.org/10.1091/mbc.E03-09-0708

Momany, M., F. Pan, and R.L. Malmberg. 2008. Evolution and conserved domains of the septins. *In* The Septins. P.A. Hall, S.E.G. Russell, and J.R. Pringle, editors. John Wiley & Sons, Ltd., Chicester, West Sussex. 35–45. http://dx.doi.org/10.1002/9780470779705.ch2

Morishita, M., and J. Engebrecht. 2008. Sorting signals within the *Saccharomyces cerevisiae* sporulation-specific dityrosine transporter, Dtr1p, C terminus promote Golgi-to-prospore membrane transport. *Eukaryot. Cell.* 7:1674–1684. http://dx.doi.org/10.1128/EC.00151-08

Muhlrad, D., R. Hunter, and R. Parker. 1992. A rapid method for localized mutagenesis of yeast genes. *Yeast.* 8:79–82. http://dx.doi.org/10.1002/yea.320080202

Nagaraj, S., A. Rajendran, C.E. Jackson, and M.S. Longtine. 2008. Role of nucleotide binding in septin-septin interactions and septin localization in *Saccharomyces cerevisiae*. *Mol. Cell. Biol.* 28:5120–5137. http://dx.doi.org/10.1128/MCB.00786-08

Nakanishi, H., M. Morishita, C.L. Schwartz, A. Coluccio, J. Engebrecht, and A.M. Neiman. 2006. Phospholipase D and the SNARE Sso1p are necessary for vesicle fusion during sporulation in yeast. *J. Cell Sci.* 119:1406–1415. http://dx.doi.org/10.1242/jcs.02841

Neiman, A.M. 2011. Sporulation in the budding yeast Saccharomyces cerevisiae. *Genetics.* 189:737–765. http://dx.doi.org/10.1534/genetics.111.127126

Nishihama, R., M. Onishi, and J.R. Pringle. 2011. New insights into the phylogenetic distribution and evolutionary origins of the septins. *Biol. Chem.* 392:681–687. http://dx.doi.org/10.1515/BC.2011.086

Oh, Y., J. Schreiter, R. Nishihama, C. Wloka, and E. Bi. 2013. Targeting and functional mechanisms of the cytokinesis-related F-BAR protein Hof1 during the cell cycle. *Mol. Biol. Cell.* 24:1305–1320. http://dx.doi.org/10.1091/mbc.E12-11-0804

Onishi, M., T. Koga, A. Hirata, T. Nakamura, H. Asakawa, C. Shimoda, J. Bähler, J.Q. Wu, K. Takegawa, H. Tachikawa, et al. 2010. Role of septins in the orientation of forespore membrane extension during sporulation in fission yeast. *Mol. Cell. Biol.* 30:2057–2074. http://dx.doi.org/10.1128/MCB.01529-09

Ozsarac, N., M. Bhattacharyya, I.W. Dawes, and M.J. Clancy. 1995. The *SPR3* gene encodes a sporulation-specific homologue of the yeast CDC3/10/11/12 family of bud neck microfilaments and is regulated by ABFI. *Gene.* 164:157–162. http://dx.doi.org/10.1016/0378-1119(95)00438-C

Pablo-Hernando, M.E., Y. Arnaiz-Pita, H. Tachikawa, F. del Rey, A.M. Neiman, and C.R. Vázquez de Aldana. 2008. Septins localize to microtubules during nutritional limitation in *Saccharomyces cerevisiae*. *BMC Cell Biol.* 9:55. http://dx.doi.org/10.1186/1471-2121-9-55

Pan, F., R.L. Malmberg, and M. Momany. 2007. Analysis of septins across kingdoms reveals orthology and new motifs. *BMC Evol. Biol.* 7:103. http://dx.doi.org/10.1186/1471-2148-7-103

Park, J.S., and A.M. Neiman. 2012. *VPS13* regulates membrane morphogenesis during sporulation in *Saccharomyces cerevisiae*. *J. Cell Sci.* 125:3004–3011. http://dx.doi.org/10.1242/jcs.105114

Potter, C.S., H. Chu, B. Frey, C. Green, N. Kisseberth, T.J. Madden, K.L. Miller, K. Nahrstedt, J. Pulokas, A. Reilein, et al. 1999. Leginon: a system for fully automated acquisition of 1000 electron micrographs a day. *Ultramicroscopy.* 77:153–161. http://dx.doi.org/10.1016/S0304-3991(99)00043-1

Rekas, A., J.R. Alattia, T. Nagai, A. Miyawaki, and M. Ikura. 2002. Crystal structure of venus, a yellow fluorescent protein with improved maturation and reduced environmental sensitivity. *J. Biol. Chem.* 277:50573–50578. http://dx.doi.org/10.1074/jbc.M209524200

Riedel, C.G., M. Mazza, P. Maier, R. Körner, and M. Knop. 2005. Differential requirement for phospholipase D/Spo14 and its novel interactor Sma1 for regulation of exocytotic vesicle fusion in yeast meiosis. *J. Biol. Chem.* 280:37846–37852. http://dx.doi.org/10.1074/jbc.M504244200

Rothman, J.H., and T.H. Stevens. 1986. Protein sorting in yeast: mutants defective in vacuole biogenesis mislocalize vacuolar proteins into the late secretory pathway. *Cell.* 47:1041–1051. http://dx.doi.org/10.1016/0092-8674(86)90819-6

Roy, A., and T.P. Levine. 2004. Multiple pools of phosphatidylinositol 4-phosphate detected using the pleckstrin homology domain of Osh2p. *J. Biol. Chem.* 279:44683–44689. http://dx.doi.org/10.1074/jbc.M401583200

Rudge, S.A., V.A. Sciorra, M. Iwamoto, C. Zhou, T. Strahl, A.J. Morris, J. Thorner, and J. Engebrecht. 2004. Roles of phosphoinositides and of Spo14p (phospholipase D)-generated phosphatidic acid during yeast sporulation. *Mol. Biol. Cell.* 15:207–218. http://dx.doi.org/10.1091/mbc.E03-04-0245

Sandrock, K., I. Bartsch, S. Bläser, A. Busse, E. Busse, and B. Zieger. 2011. Characterization of human septin interactions. *Biol. Chem.* 392:751–761. http://dx.doi.org/10.1515/BC.2011.081

Sellin, M.E., S. Stenmark, and M. Gullberg. 2012. Mammalian SEPT9 isoforms direct microtubule-dependent arrangements of septin core heteromers. *Mol. Biol. Cell.* 23:4242–4255. http://dx.doi.org/10.1091/mbc.E12-06-0486

Sikorski, R.S., and P. Hieter. 1989. A system of shuttle vectors and yeast host strains designed for efficient manipulation of DNA in *Saccharomyces cerevisiae. Genetics.* 122:19–27.

Sirajuddin, M., M. Farkasovsky, F. Hauer, D. Kühlmann, I.G. Macara, M. Weyand, H. Stark, and A. Wittinghofer. 2007. Structural insight into filament formation by mammalian septins. *Nature.* 449:311–315. http://dx.doi.org/10.1038/nature06052

Sirajuddin, M., M. Farkasovsky, E. Zent, and A. Wittinghofer. 2009. GTP-induced conformational changes in septins and implications for function. *Proc. Natl. Acad. Sci. USA.* 106:16592–16597. http://dx.doi.org/10.1073/pnas.0902858106

Suda, Y., R.K. Rodriguez, A.E. Coluccio, and A.M. Neiman. 2009. A screen for spore wall permeability mutants identifies a secreted protease required for proper spore wall assembly. *PLoS One.* 4:e7184. http://dx.doi.org/10.1371/journal.pone.0007184

Tartof, K.D., and C.A. Hobbs. 1987. Improved media for growing plasmid and cosmid clones. *Bethesda Res. Lab Focus.* 9:12–14.

Taylor, D.W., D.F. Kelly, A. Cheng, and K.A. Taylor. 2007. On the freezing and identification of lipid monolayer 2-D arrays for cryoelectron microscopy. *J. Struct. Biol.* 160:305–312. http://dx.doi.org/10.1016/j.jsb.2007.04.011

Varma, A., E.B. Freese, and E. Freese. 1985. Partial deprivation of GTP initiates meiosis and sporulation in *Saccharomyces cerevisiae. Mol. Gen. Genet.* 201:1–6. http://dx.doi.org/10.1007/BF00397977

Versele, M., and J. Thorner. 2004. Septin collar formation in budding yeast requires GTP binding and direct phosphorylation by the PAK, Cla4. *J. Cell Biol.* 164:701–715. http://dx.doi.org/10.1083/jcb.200312070

Versele, M., B. Gullbrand, M.J. Shulewitz, V.J. Cid, S. Bahmanyar, R.E. Chen, P. Barth, T. Alber, and J. Thorner. 2004. Protein-protein interactions governing septin heteropentamer assembly and septin filament organization in *Saccharomyces cerevisiae. Mol. Biol. Cell.* 15:4568–4583. http://dx.doi.org/10.1091/mbc.E04-04-0330

Weems, A.D., C.R. Johnson, J.L. Argueso, and M.A. McMurray. 2014. Higher-order septin assembly is driven by GTP-promoted conformational changes: evidence from unbiased mutational analysis in *Saccharomyces cerevisiae. Genetics.* 196:711–727. http://dx.doi.org/10.1534/genetics.114.161182

Weirich, C.S., J.P. Erzberger, and Y. Barral. 2008. The septin family of GTPases: architecture and dynamics. *Nat. Rev. Mol. Cell Biol.* 9:478–489. http://dx.doi.org/10.1038/nrm2407

Westfall, P.J.J.C., J.C. Patterson, R.E. Chen, and J. Thorner. 2008. Stress resistance and signal fidelity independent of nuclear MAPK function. *Proc. Natl. Acad. Sci. USA.* 105:12212–12217. http://dx.doi.org/10.1073/pnas.0805797105

Wittinghofer, A., and I.R. Vetter. 2011. Structure-function relationships of the G domain, a canonical switch motif. *Annu. Rev. Biochem.* 80:943–971. http://dx.doi.org/10.1146/annurev-biochem-062708-134043

Zhang, J., C. Kong, H. Xie, P.S. McPherson, S. Grinstein, and W.S. Trimble. 1999. Phosphatidylinositol polyphosphate binding to the mammalian septin H5 is modulated by GTP. *Curr. Biol.* 9:1458–1467. http://dx.doi.org/10.1016/S0960-9822(00)80115-3